Outcrop Analog

for

Lower Paleozoic Hydrothermal Dolomite Reservoirs,

Mohawk Valley, NY

A thesis presented to the Faculty

of the University at Albany, State University of New York

in partial fulfillment of the requirements

for the degree of

Master of Science

College of Arts & Sciences

Department of Geology

Brian E. Slater
2007

Abstract

Geochemical analysis and field relations of linear dolomite bodies occurring in outcrop in the Mohawk Valley of New York suggest that they have undergone significant fault-related hydrothermal diagenesis. This study uses fluid inclusions, stable isotopes, 3D-Ground penetrating radar, core analysis, and surficial observation which all show a link between faulting, dolomitization, and other hydrothermal alteration. The outcrop is a scaled analog for Trenton - Black River hydrothermal dolomite reservoirs of the eastern United States.

The study site occurs in the Lower Ordovician Tribes Hill Formation, which is an early Ordovician shaley limestone. The outcrop has an en echelon fault, fracture and fold pattern. A 3-D ground penetrating radar survey of the quarry floor has helped to map out faults, fractures, anticlines, synclines and the extent of dolomitization. Most of the dolomitization occurs in fault-bounded synclines or “sags” flanked by anticlines. The dolomite structures are highly localized, occurring around faults and are absent away from the faults and fractures. Trenches cut across the outcrop help relate offset along faults to the overall geometry of the dolomitized bodies. Geochemical analysis, though helpful in characterizing the conditions of dolomitization, do not define its origin absolutely. Although the outcrop is much too small and shallow to act as a producing gas field, it may be studied as a scaled analog to help petroleum geologists characterize existing gas plays and prospect future areas of exploration.

Acknowledgements

Although the requirements for this thesis are designed as a two year project, the study of the Palatine Bridge outcrop has been an ongoing task for the last four years. Throughout this time period, many people and organizations have gotten involved and must therefore be acknowledged.

A sincere thanks to:

Everyone at the Reservoir Characterization Group of the New York State Museum for their manual labor in the excavation process, sample collection, fracture mapping, and work on the trenches. (Justin Deming, Lauren Hall, Eric Hawkins, Brian Hupe, Jim Leone, Matt Montario, Richard Nyahay, Mike Pascucci, Jim Sandor, Rose Schulze, and Don Thompson)

Rick Bray for his core analysis and help with the thin section interpretations and digenetic processes.

Steve Howe at the University of Albany for his help with the fluid inclusion analyses and work on the stable isotopes

Mark Grasmeuk and Dave Viggiano for conducting the ground penetrating radar survey and processing the data

Greg Piascik, Scott Misener, and Joe SantaMaria at the Department of Transportation for drilling the cores on the coldest week in past 5 years

Fluid Inclusion Technologies for running analyses on the first two inclusion samples

Mihai Ducea at the University of Arizona for doing the Sr isotope analyses

Eagle Associate Concrete Company for cutting the trenches

Ansbro Petroleum Company, Columbia Natural Resources, Fortuna Energy, and John Martin at NYSERDA, for funding this very expensive thesis project

Harold Brossman, the care-taker of the quarry, for allowing us to conduct our study on the premises

Gareth Cross for his initial discovery of the outcrop without which this study would not have been possible

And finally Dr. Langhorne “Taury” Smith and Richard Nyahay of the Reservoir Characterization Group at the New York Museum for their continual guidance, support, and supervision

Table of Contents

List of Tables

List of Figures

List of Plates

Chapter 1 – Introduction

1.1. Aims and objectives of the investigation

The goal of this investigation was to test the hypothesis that dolomitization and associated mineralization of the Tribes Hill Limestone in Palatine Bridge, NY was caused by hydrothermal[1] fluid flow upward along faults and fractures. It may therefore be used as an outcrop analog for the Trenton - Black River dolomite gas fields on the basis of their similar origin and comparable features. This study addresses three objectives:

1) Confirm hydrothermal origin of the Palatine Bridge outcrop

2) Constrain timing of dolomitization

3) Confirm value of the outcrop as an analog for Trenton - Black River fields

An assessment of how well the study meets these objectives is presented in Chapter 6.

[1] For the purposes of this paper hydrothermal fluids are defined as "aqueous solutions that are warm or hot relative to the surrounding environment" whereby temperature differences greater than 10°C are considered significant (White, 1957).

1.2. Association of Hydrothermal Dolomite with Gas Production

Although detailed research of its formation is relatively young, hydrothermal dolomite has long been associated with the production of natural gas. In 1884 North America experienced its first real drilling boom along the Indiana-Lima trend of Indiana and Ohio (Hurley and Budros, 1990). Large amounts of both oil and gas were produced from the Ordovician-aged Trenton-Black River units. According to Keith (1986) half of the area's production came from the Bowling Green fault zone, a highly dolomitized linear feature.

In 1957/1958 the Albion-Scipio fields were discovered along a similar Trenton-Black River dolomitized fault trend in Michigan (Fig. 1). With over 400 producing wells by 1961, this system was among the first to achieve the status of giant oil field. The fields' linear geometry and synclinal sags led to the interpretation that these features were created by hydrothermal fluid flow along riedel shears in a strike-slip pull-apart system (Fig. 2) (Hurley and Budros, 1990).

Since the discovery of these early fields, hydrothermally dolomitized sections of the Trenton-Black River have been proven to host some of the largest natural gas wells in the world (Smith, 2006). Fields such as the Rochester Field in southern Ontario and the Quakenbush Hill Field in south central New York produce from these localized dolomite bodies. Fields of this type are characterized by their long, linear shape, close proximity to fault zones, breccias, vugs, and central depressions or sags (Smith, 2006).

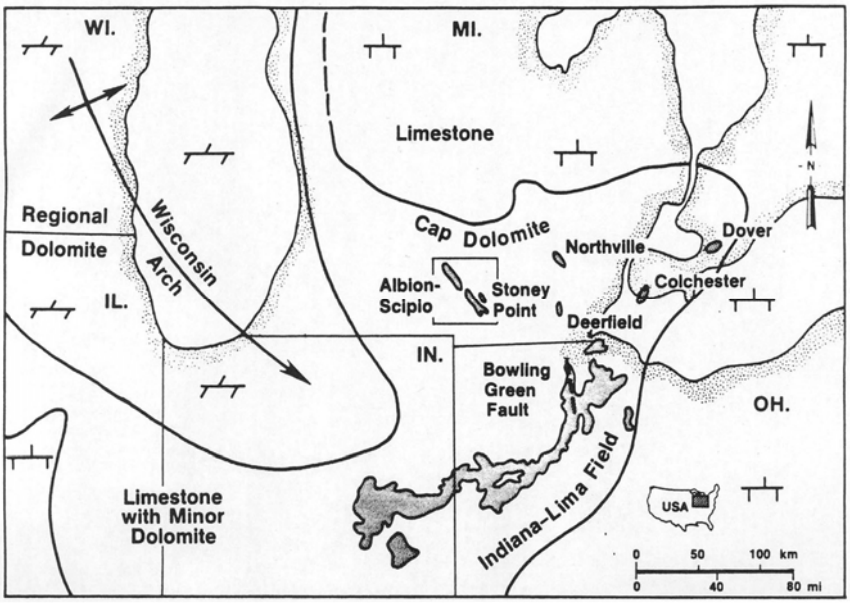

Figure 1 – Map outlining early oil and gas fields of the Great Lakes Region
(Hurley and Budros, 1990)

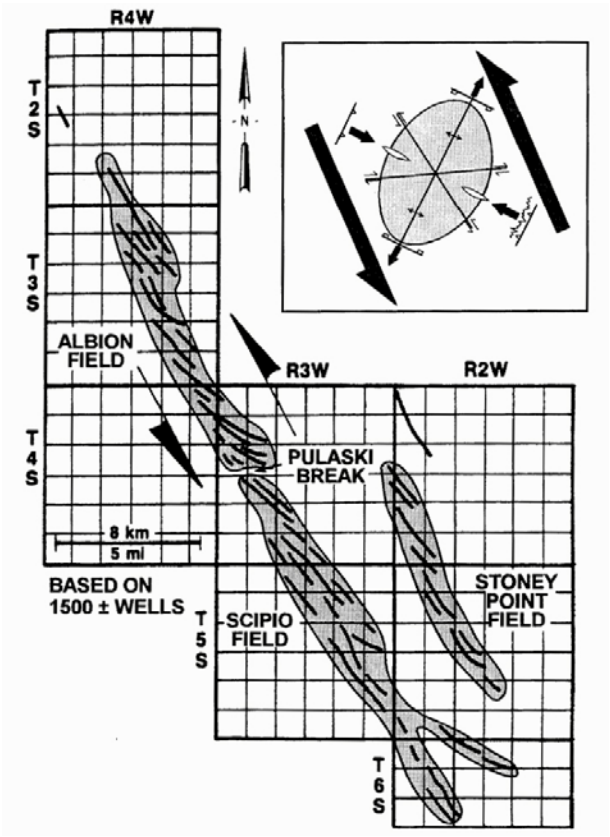

Figure 2 - Interpreted strike-slip motion of the Albion-Scipio fields
(Hurley and Budros, 1990)

1.3. Fault-related Hydrothermal Alteration Model

The current model for fault-related hydrothermal alteration is based on the research done by Davies and Smith (2006). The process begins with the activation of basement-rooted faults. This may involve the reactivation appropriately oriented pre-existing faults or the creation of entirely new ones (Sibson, 1994). Movement along strike-slip and transtensional faults can create a relatively low-resistance flow path for high-pressure, high-temperature fluids trapped at greater depths. The release of this pressure causes the fluids to travel upward along fault planes where they interact with the units above. This faulting is commonly transtensional in nature creating negative flower structures which are characterized by sagging. In the case of interaction with limestone, as the fluids cool they become under-saturated with respect to calcite and begin to leach the host rock creating secondary porosity in the form of vugs. Increased permeability created by the leaching process allows fluids to migrate farther away from the fault zone. The pressure and temperature change associated with these fluids traveling to shallower depths can also cause them to become super-saturated with dolomite, leading to precipitation of the mineral as both matrix replacement and vug and fracture fill. The evolution of these fluids can lead to the precipitation of a range of other minerals as well. Quartz, bitumen, pyrite and secondary calcite are all associated with hydrothermal alteration. Mineralization along faults and fractures may choke the flow path and cause fluid travel to cease (Sibson, 1994). However, continued tectonic activity and the build-up of pressure may reactivate these passage ways and initiate another dolomitization event.

1.4. Brief Description of Palatine Bridge Outcrop

The Palatine Bridge study site is located in the Frye Estate quarry along the Mohawk River, approximately 50 miles west of Albany, NY (Fig. 3). Although at least three areas of the quarry have been dolomitized, this study focuses on the most easily accessible region (Fig 4). The study area consists of two dolomite bodies. The easternmost body (Body 1) is a long, linear feature approximately 55 feet long, 5 feet wide, and has a strike of 305°. The second body (Body 2) is located immediately west of the first, and is also a linear feature with similar strike, however this body is substantially longer than the first, measuring 110 feet Body 2 is broken into two parts which are separated by a southerly bend, referred to as the "jog."

The dolomite is easily distinguished from the surrounding limestone by its distinct orange color and massive texture. The bodies are characterized by their central sag, brecciation, and vuggy porosity. An intense fracture zone surrounds the entire outcrop increasing the width of the affected area to approximately 15 feet. Although it is tens of times smaller than producing hydrothermal reservoirs, the quarry outcrop bares a striking resemblance to them in every other way. This suggests that the outcrop may be studied as a small-scale analog of the larger, deeply buried Trenton-Black River fields.

Figure 3 - Satellite image of New York State with Palatine Bridge Quarry location marked

Figure 4 - Panorama view of Palatine Bridge Quarry outcrop
(taken from the south looking north)

Chapter 2 – Background

2.1. Site Location

The Palatine Bridge Outcrop is located in Central New York, along the Mohawk River Valley. It lies on the floor of the Frye Estate Quarry which is situated on the western edge of town along Route 5. The Mohawk River runs along the strike of the bodies only a few hundred feet south of the quarry's edge. Access to the quarry is limited as it has been inactive since the 1970's when it supplied aggregate for the construction of Interstate 90.

2.2. Stratigraphic Setting

The Palatine Bridge quarry is in the Lower Ordovician Tribes Hill Formation of the Beekmantown Group (Fig. 5 and 6). Fisher (1954), Zenger (1981), and Landing et al. (1996) describe the Tribes Hill as a thin to medium-bedded argillaceous limestone which was deposited in a shallow, peritidal to subtidal environment. It is characterized by blackish laminae and shaley interbeddings. The formation has a regional thickness of about 130 feet. It is considered fossiliferous for its abundance of trilobite, brachiopod, and mollusk faunas (Landing, 1996). The Tribes Hill unconformably overlies the Upper Cambrian Little Falls Formation which is described as a thick-bedded dolostone and is also believed to have formed by deposition in a shallow, peritidal to subtidal environment (Zenger, 1981). According to Zenger, the Little Falls is approximately 400 feet thick in

this portion of the Mohawk Valley. The Little Falls overlies the Potsdam sandstone which may or may not be present below the quarry as it thins to the east.

The Tribes Hill Limestone is capped by the knox unconformity which accounts for approximately 30 million years of absent strata. Above this unconformity lies the Upper Ordovician Trenton - Black River Group and the Utica Shale, however these units are absent from the Palatine Bridge quarry as they have been eroded away. The Trenton and Black River units are well known for their oil and gas plays along the eastern portion of the US and into southern Ontario. The majority of these plays are contained in hydrothermal dolomite reservoirs (Smith, 2006).

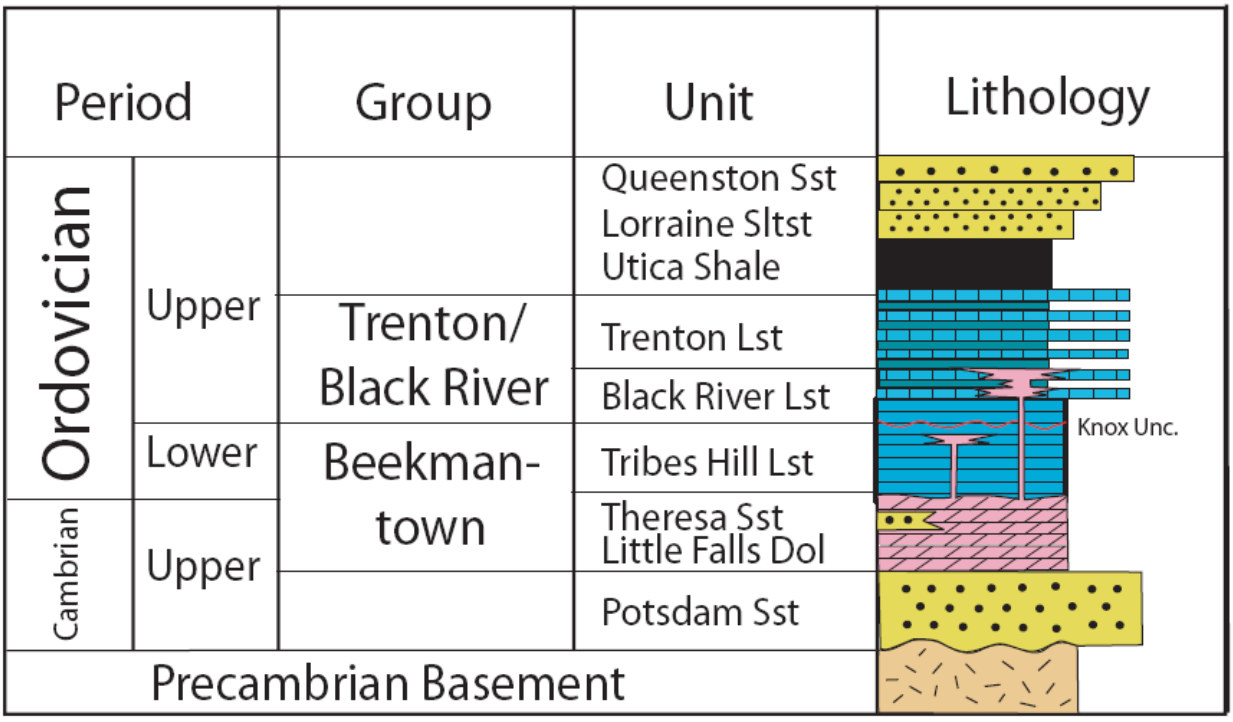

Figure 5 - Stratigraphic column of the Precambrian through Ordovician (Smith 2006)

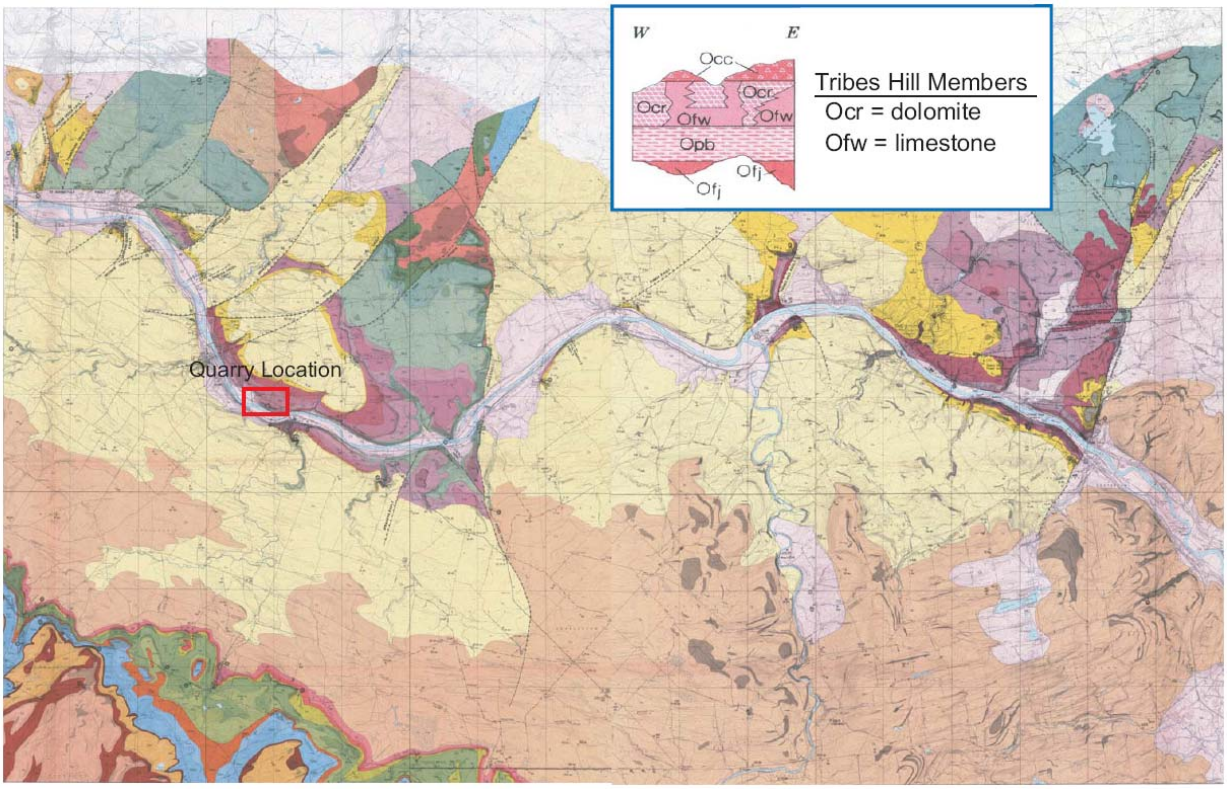

Figure 6 - Quarry Location plotted on geologic map of the Mohawk Valley (Fisher, 1980)

2.3. Tectonic Setting

The basement rock of New York State consists mainly of granitic gneiss. It is part of the Grenville Province which formed approximately 1.1 billion years ago during the Grenville Orogeny. These rocks remained relatively undisturbed until the end of the Precambrian (660 Ma) when rifting led to the opening of the Iapetus Ocean and reactivated preexisting faults in the basement (Jacobi and Fountain, 2002). Deposition of the Potsdam Sandstone and Beekmantown Group during the Late Cambrian and Early Ordovician is believed to have occurred along a passive margin following the opening the Iapetus Ocean. Conversely, deposition of the Middle Ordovician Trenton - Black River

Group has been demonstrated to have been fault controlled (Bradley and Kidd, 1991; Joy et al., 2000). Active tectonism during the Middle-Late Ordovician is associated with the Taconic Orogeny in which Proto-North America collided with the Taconic Island Arc terrain. Flexure of the North American plate during its attempt to be subducted under the island arc led to extensional faulting and produced a series of north east-south west striking normal faults, some with offsets of over 1000 feet (Jacobi, 1981; Bradley and Kidd, 1991). Closing of the Iapetus Ocean during the Devonian (410 – 380 Ma) caused a transform collision between proto-North America and Avalon known as the Acadian Orogeny. The last orogeny recorded in New York took place during the Late Carboniferous and Early Permian (330 – 250 Ma). This transform collision involved a portion of proto-Africa being accreted to eastern proto-North America. This event is known as the Alleghanian Orogeny.

Chapter 3 – Fieldwork and Methods

In order to fulfill the objectives set out in Chapter 1, analysis of the outcrop was performed using several different geological disciplines.

3.1. Excavation

The Palatine Bridge outcrop was initially discovered by Gareth Cross, a master's student from the University of Buffalo. While mapping fractures in the Mohawk Valley, he noted the orange-colored rubble on the floor of the quarry. Very few pieces of in-situ dolomite could be seen (Fig. 7).

The quarry floor was initially covered by 2-3 feet of over overburden. Excavation began with the use of pick-axes and shovels, but it was soon realized that more effective machinery would be needed to efficiently expose the outcrop. A dingo (walk behind bucket-loader) and a Caterpillar (skid-steer bucket loader) were rented from local tool stores and used to push aside the overburden and expose the dolomite bodies.

High-pressure hoses were then used to pump water from a nearby pond and spray off the outcrop. This served to remove the remaining debris and wash the in-situ formation. The excavation was followed by extensive photography both on the ground and from a 60 foot boom (Plate 1).

Figure 7 - Dolomite exposure prior to excavation

3.2. 3-D Ground Penetrating Radar

During the excavation process, while much of the outcrop was still covered by overburden, a three dimensional ground penetrating radar survey was run over the area. Mark Grasmuek and his student David Viggiano, from the University of Miami, conducted the survey. Data was collected using a shielded bistatic 250 MHz antennae, then processed using Promax 3D™ and Geoprobe™ software. Two survey sites were selected based on surficial observations. The first site was located in the area being excavated and only covered Body 2 since Body 1 had already been exposed (Fig. 8). The second site was located in a different part of the quarry approximately 50 feet higher in elevation. This second site was chosen based on the presence of dolomite rubble and because a preliminary 2-D run showed structure in the area. Results from the survey of the first site are presented in Chapter 4.

Figure 8 - Outline of 3-D survey area

3.3. Drill Cores

In January of 2005 the Department of Transportation was contracted to drill a series of six 2 inch cores in the study area. These holes ranged in depth from 38 to 73 feet. Figure 9 shows a map of the hole locations and total depths of all the holes are given in Table 1. Hole 1 was drilled approximately half way between the jog and the eastern tip of Body 2. Holes 2 and 6 are located 5 and 15 feet outside Body 2 along a line drawn perpendicular to strike from Hole 1. Hole 5 was drilled inside the jog of Body 2. Hole 3 was located at the eastern tip of Body 2 while Hole 4 was drilled in the limestone gap between bodies 1 and 2. All six cores were slabbed and boxed for storage before analysis.

Figure 9 - Map of core drilling locations

Table I – Core holes and their corresponding total depths

Hole #	Total Depth (ft.)
1	38.8
2	54.0
3	55.0
4	55.0
5	73.0
6	45.0

3.4. Fracture Mapping

A fracture map covering the entire exposure was constructed using a 2 feet x 10 foot grid broken into five 2 foot squares with durable string. The grid was weighted on both ends and placed over the eastern end of the first body. The fracture content of each square was then drawn to scale on a sheet of graph paper. Once the row of squares were completely copied, the eastern end of the grid was "flipped" over to cover the adjacent row of outcrop. The new row of squares was then copied and this flipping process was repeated. The entire outcrop was mapped in this fashion, then scanned and digitized. A copy of the finished map is presented in Plate 2.

3.5. Trenches

During the summer of 2005 Eagle Associates Concrete Cutting Company was contracted to cut six trenches across the dolomite bodies (Fig. 10). The location of each trench is given in Figure 11. These trenches each measure approximately 3 feet wide, 15 feet long, and 18 inches deep. The perimeter cuts for each trench were made using a 36-

inch rail-mounted circular wet saw. Once the cuts had been made, a jackhammer was used to break apart the interior for removal. A series of digital photographs were taken of each trench wall and seamed together to make mosaic cross-sections of each trench. A full description of these cross-sections is given in Chapter 4.

Figure 10 - One of the six trenches cut across the dolomite bodies (trench 4 looking west)

Figure 11 - Map of trench locations

3.6. Sample Collection and Geochemical Analysis

Samples of the outcrop were collected at various times throughout its excavation. The initial set consisted of 18 samples in and around the dolomite bodies. These samples were removed using a rock hammer and therefore have no consistent size or shape. Later, two more series of samples were collected using a Pomeroy EZ core plugger. Each plug

is a cylinder with a 1-inch diameter and a length varying from 1 to 3 inches. A set of plugs were taken along the bodies every two feet. Another set of plugs were taken as a transect cutting across the eastern portion of Body 2. A fourth set was collected from the cores using a drill press mounted with the same type bit as the plugger. Samples were taken from the cores every two feet starting from the surface and ending at the Tribes Hill / Little Falls contact. A portion of each sample was sent to Spectrum Petrographics in Washington to be made into thin sections. The remainder of some samples were crushed to a fine powder, then divided and sent to Steven Howe at the University of Albany for stable isotope analysis and to Mihai Ducea at the University of Arizona for strontium isotope analysis.

Stable isotopes of carbon and oxygen were measured at the University of Albany, NY. In each case approximately 200 mg of powdered sample was dissolved in 100% phosphoric acid at 90°C in individual reaction vessels in a MultiPrep sample preparation device. The evolved CO_2 gas was then analyzed using a Micromass Optima gas-source triple-collector isotope ratio mass spectrometer. Samples of international standard NBS-19 were interspersed among the shell samples in analytical runs. All carbon and oxygen isotopic compositions are reported as per mil deviations relative to Vienna Peedee belemnite (VPDB).

Strontium isotope ratios were acquired at the University of Arizona using a VG Sector 54 multi-collector TIMS instrument fitted with adjustable 10^{11} Ω Faraday collectors and Daly photomultipliers. Multiple analyses of standard SRM 987 were used for calibration and δ^{87}Sr values are reported as the actual ratio of ^{87}Sr to ^{86}Sr.

3.7. Fluid Inclusions

Two sets of fluid inclusion analyses were performed on various samples taken from the quarry. The first set consisted of two samples taken from the floor of the quarry. They were sent to Fluid Inclusion Technologies, Inc. where doubly polished thick sections were prepared then analyzed using a USGS type heating-freezing stage. Samples were heated by passing nitrogen through a heating element and then over the sample, located in a special chamber designed to minimize lateral and vertical thermal gradients. A similar process was used for freezing the samples, however gas from the liquid nitrogen dewar was not heated before entering the sample chamber. Both homogenization temperatures (T_H) and freezing temperatures (T_F) were recorded to the nearest degree Celsius and salinities were reported to the nearest 0.1 weight percent. Primary and secondary/pseudo-secondary inclusions were studied.

A second set of samples was collected and analyzed at the University of Albany using a similar USGS type heating-freezing stage. Ten samples were taken from various locations. Three sections were made from mineralization occurring in dolomite/calcite veins in the fracture zone surrounding the outcrop. Two samples of the outcrop were collected from the dolomite bodies on quarry floor and two samples were taken from the interior of vugs lined with saddle dolomite crystals. Three matrix dolomite sections were made from core plugs at intervals where grain-texture was most coarse. A total of 41 fluid inclusions were located and analyzed in this second set. Results from both studies are presented in Chapter 4.

Chapter 4 – Data

4.1. 3-D Ground Penetrating Radar

Because the GPR survey was done before the outcrop was fully exposed, its main purpose was to aid in directing the excavation process. However, not only did the radar results help pinpoint the dolomite bodies beneath the talus, they also gave an excellent cross-section of the bodies' structure at depth. Figure 12 shows a horizontal slice from the 3-D survey (map view). This image clearly shows Body 2 including the jog. Notice the sharp contact between the structure of the body and the relatively flat lying unaltered limestone of the Tribes Hill. Figure 13 shows a vertical slice of the survey (profile view) taken across the eastern portion of Body 2. Here the body appears as a sag which is flanked by anticlines on either side. This image shows that the feature is not just a surface expression but extends through the maximum depth of the survey. Due to uncontrollable circumstances such as wet soil and clay-rich inter-beddings, the radar signal was dampened and only penetrated to a depth of about five feet

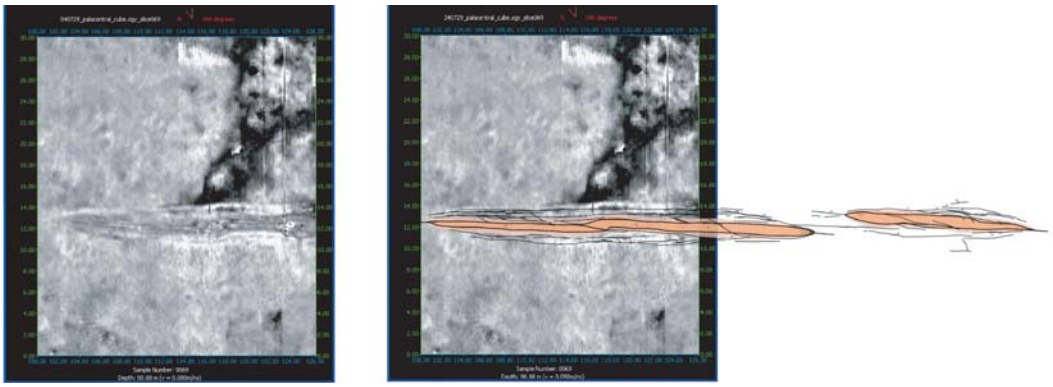

Figure 12 - Horizontal slice from Ground Penetrating Radar Survey,
and same image with fracture map overlay

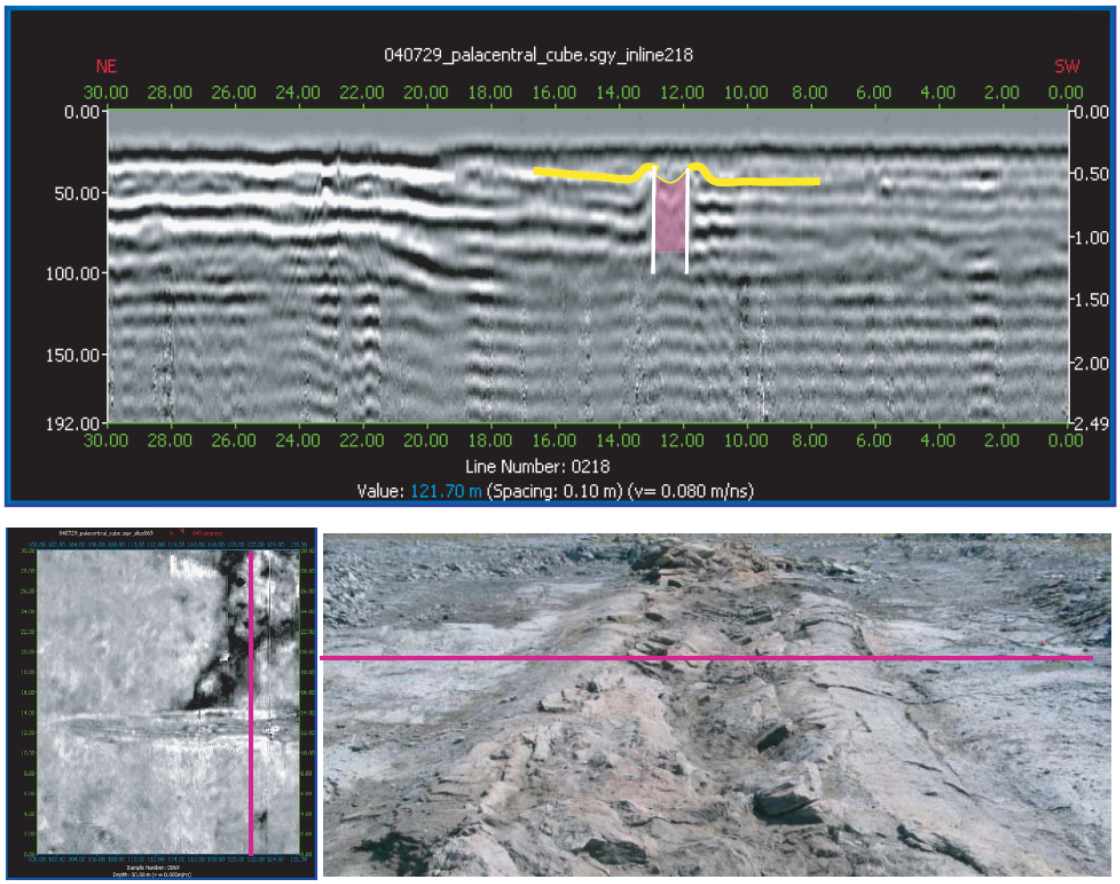

Figure 13 - Vertical slice from Ground Penetrating Radar Survey with reference lines drawn on horizontal slice and outcrop photo

4.2. Drill Cores

The six cores taken from the quarry were described by Richard D. Bray at the New York State Museum. A summary of his findings follow and the complete descriptions are available in Appendix 1. Figures 14 through 19 show stratigraphic columns for each of these core descriptions.

Hole 1 is located inside the eastern portion of Body 2 and is dolomitized throughout its entire length. The upper 12 feet of the core has well-developed intercrystalline and vuggy porosity and contains a 3 feet fracture zone with well-defined breccia clasts. The next 11 feet of core contain less porosity, but have an increased pyrite and bitumen content. The Tribes Hill / Little Falls contact occurs at a depth of 22.5 feet The remaining 15 feet of core contain pyrite and bitumen-filled fractures as well as a modeled red marker bed at 35 feet.

Hole 2 is located in the fracture zone approximately five feet north of Hole 1. The uppermost 12.6 feet of core are described as a dolomitic limestone. This zone contains three saddle dolomite-filled fractures at three, six, and seven feet Between 12 and 16 feet the core grades into a slightly calcitic dolostone taking on the characteristics of the cores drilled within the dolomite bodies. The upper four feet of this zone has well-developed intercrystalline, intergranular, and vuggy porosity. The lower three feet of the Tribes Hill contains sparse vuggy porosity, rare pyrite, and a high angle bitumen-filled fracture which continues into the Little Falls Formation. A modeled red marker bed occurs at 35 feet.

Hole 3 is located at the eastern tip of Body 2 and is dolomitized throughout its entire length. The upper seven feet of the core are characterized by numerous breccia clasts, but rare porosity. Below this interval the remaining section of Tribes Hill contains zones of densely concentrated microstylolites, excellent intercrystalline and vuggy porosity, rare pyrite, and some bitumen. The contact between the Tribes Hill and Little Falls formations occurs at approximately 25 feet below which bitumen and dolospar-filled fractures can still be observed. A modeled red marker bed occurs at 35 feet.

Hole 4 is located in the limestone gap or "bridge" between Bodies 1 and 2. The upper three feet of this core are a slightly dolomitic limestone in which the characteristics of unaltered Tribes Hill are preserved. However, the core grades into a dolostone and displays the characteristics as the dolomite bodies. From 3 to 23 feet vuggy and intercrystalline porosity increase and brecciation occurs throughout. The Tribes Hill / Little Falls contact is at approximately 24 feet A modeled red marker bed occurs at 35 feet.

Hole 5 is located in the "jog" at the center of Body 2 and is dolomitized throughout its entire length. The upper three feet of core does not show any porosity, however the remainder of the Tribes Hill section consists of zones ranging from sparse to excellent vuggy and intercrystalline porosity occurring near faults and in areas of brecciation. Beds often appear distorted by soft sediment deformation. The Tribes Hill / Little Falls contact is at approximately 24 feet A modeled red marker bed occurs at 35 feet.

Hole 6 is located outside the fracture zone approximately 15 feet north of Hole 1. The Tribes Hill section of the core spans 25 feet from the surface to Little Falls contact and is a slightly dolomitic limestone throughout. There is rare pyrite and no faults, brecciation, or visible porosity. Bedding near the bottom of the section appears to have been affected by soft sediment deformation. Within the Little Falls Formation a modeled red marker bed occurs at 35 feet.

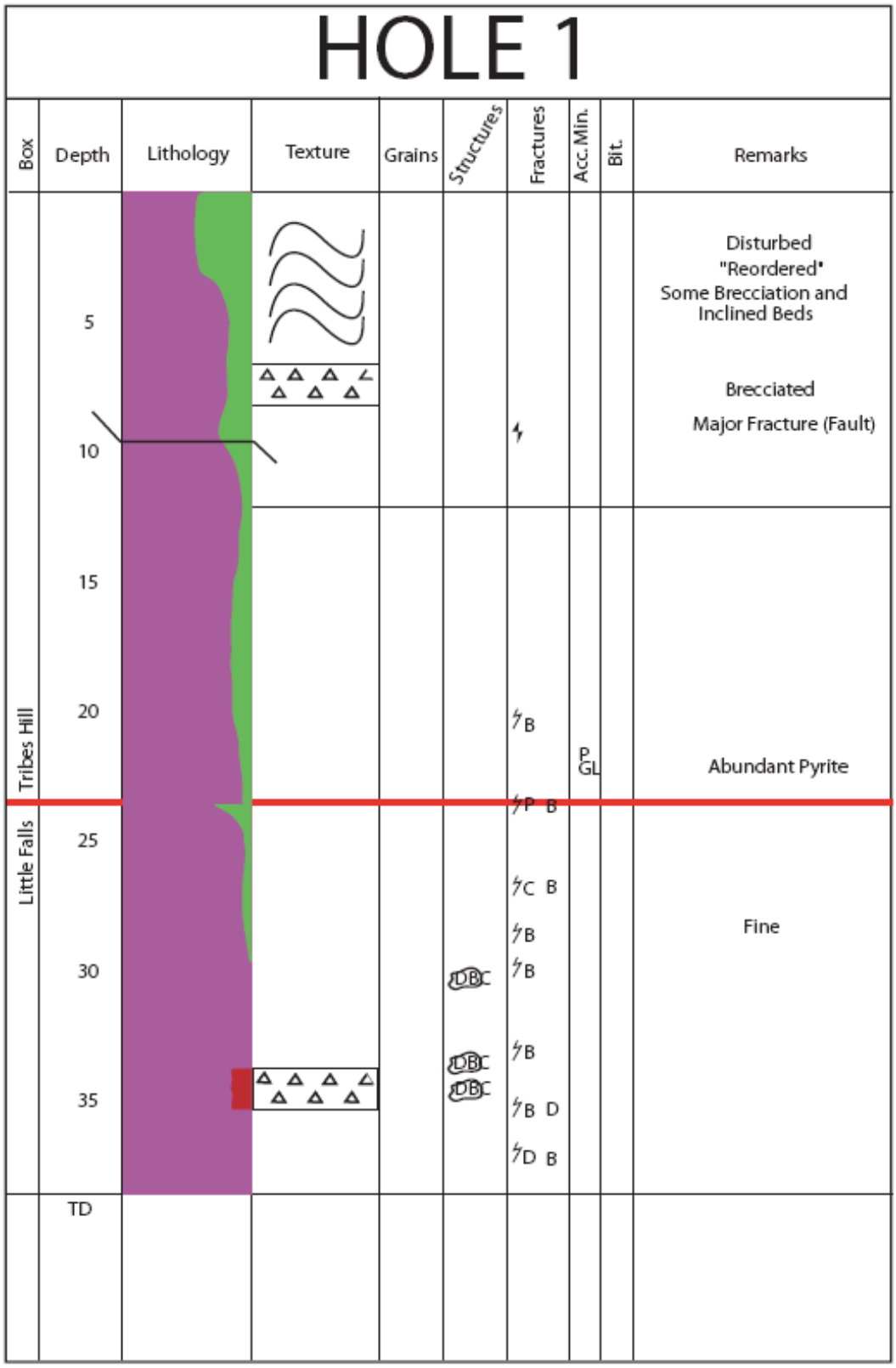

Figure 14 - Hole 1 stratigraphic column with description (digitized from Bray)

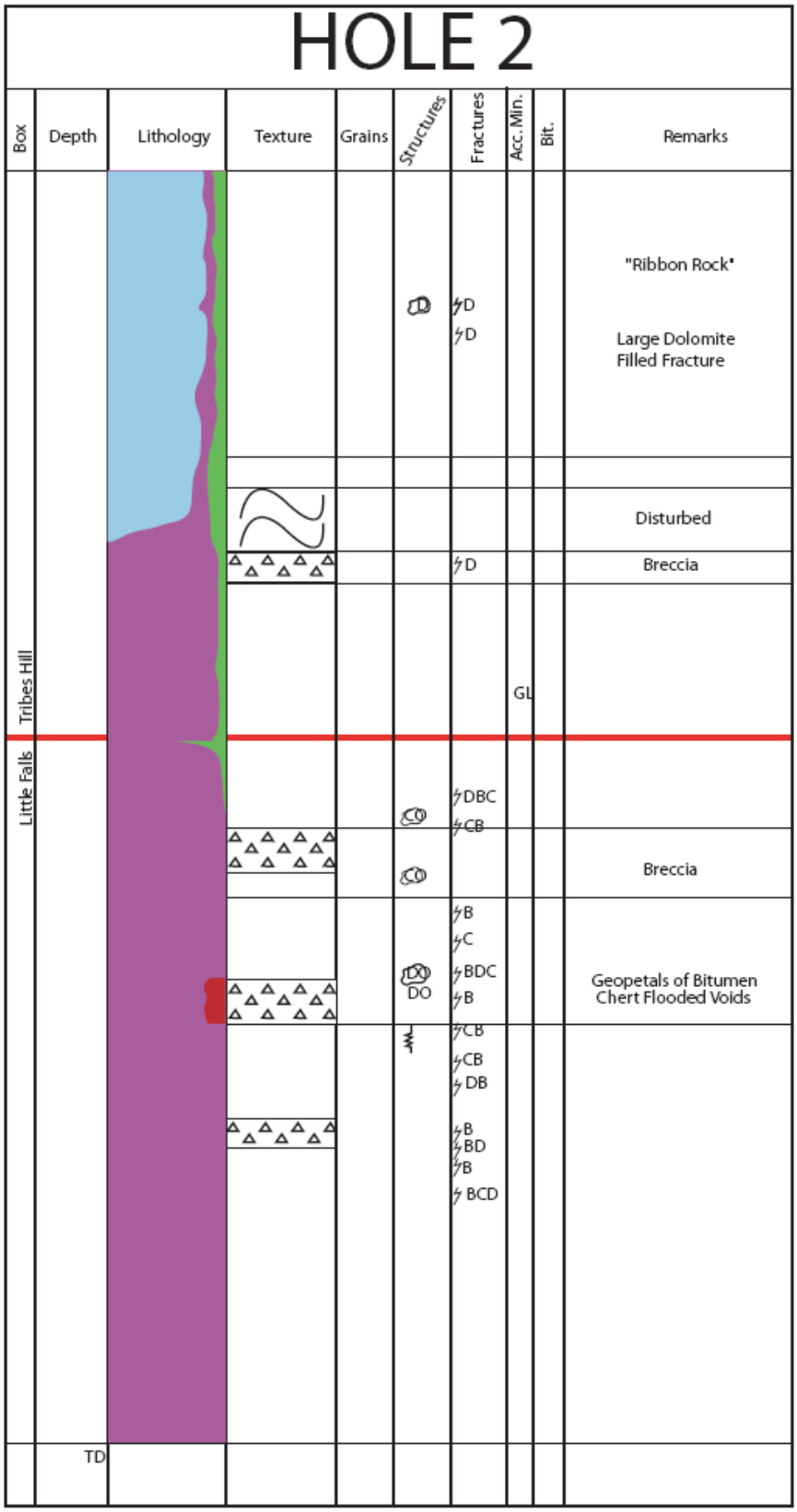

Figure 15 - Hole 2 stratigraphic column with description (digitized from Bray)

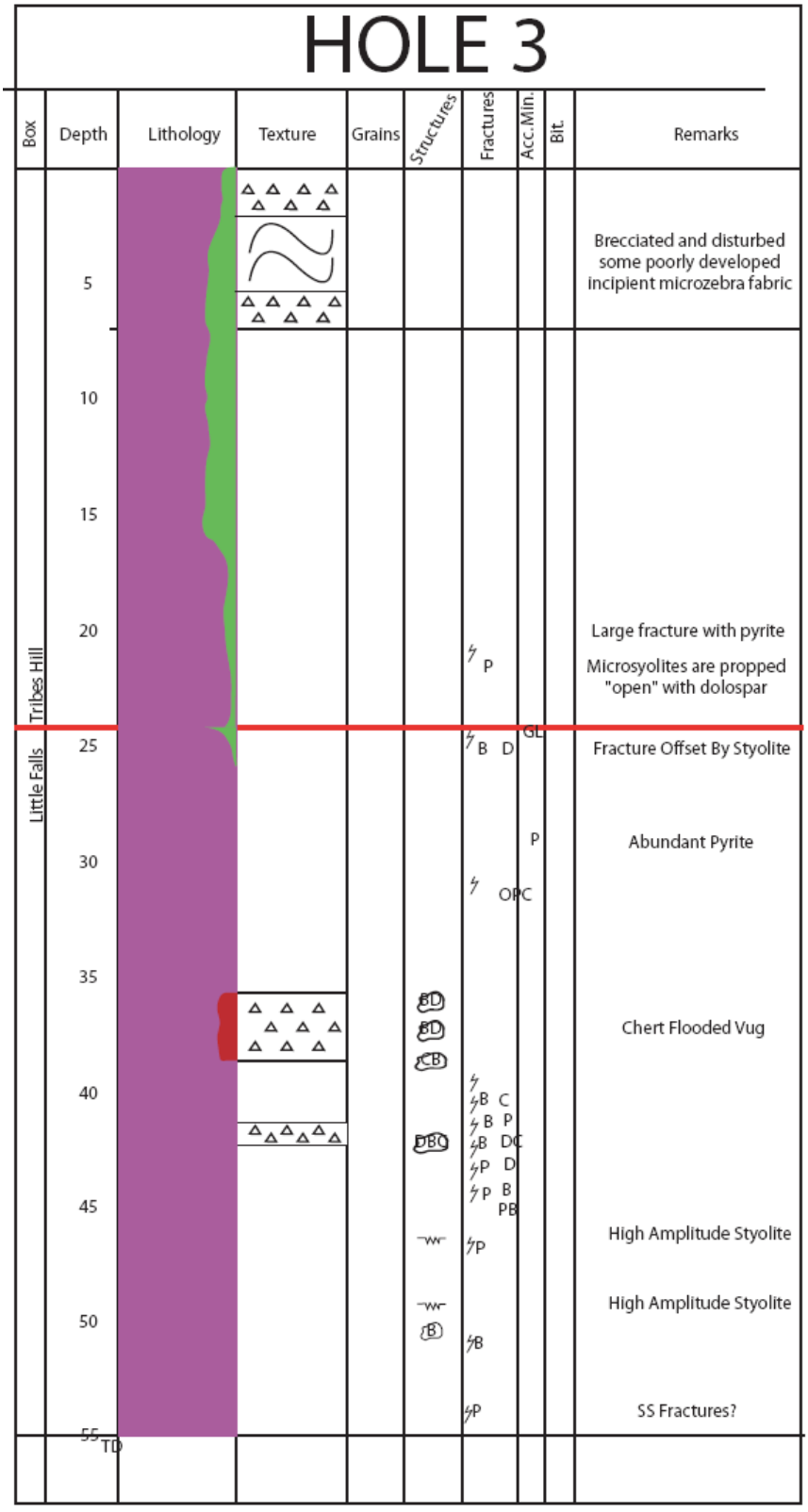

Figure 16 - Hole 3 stratigraphic column with description (digitized from Bray)

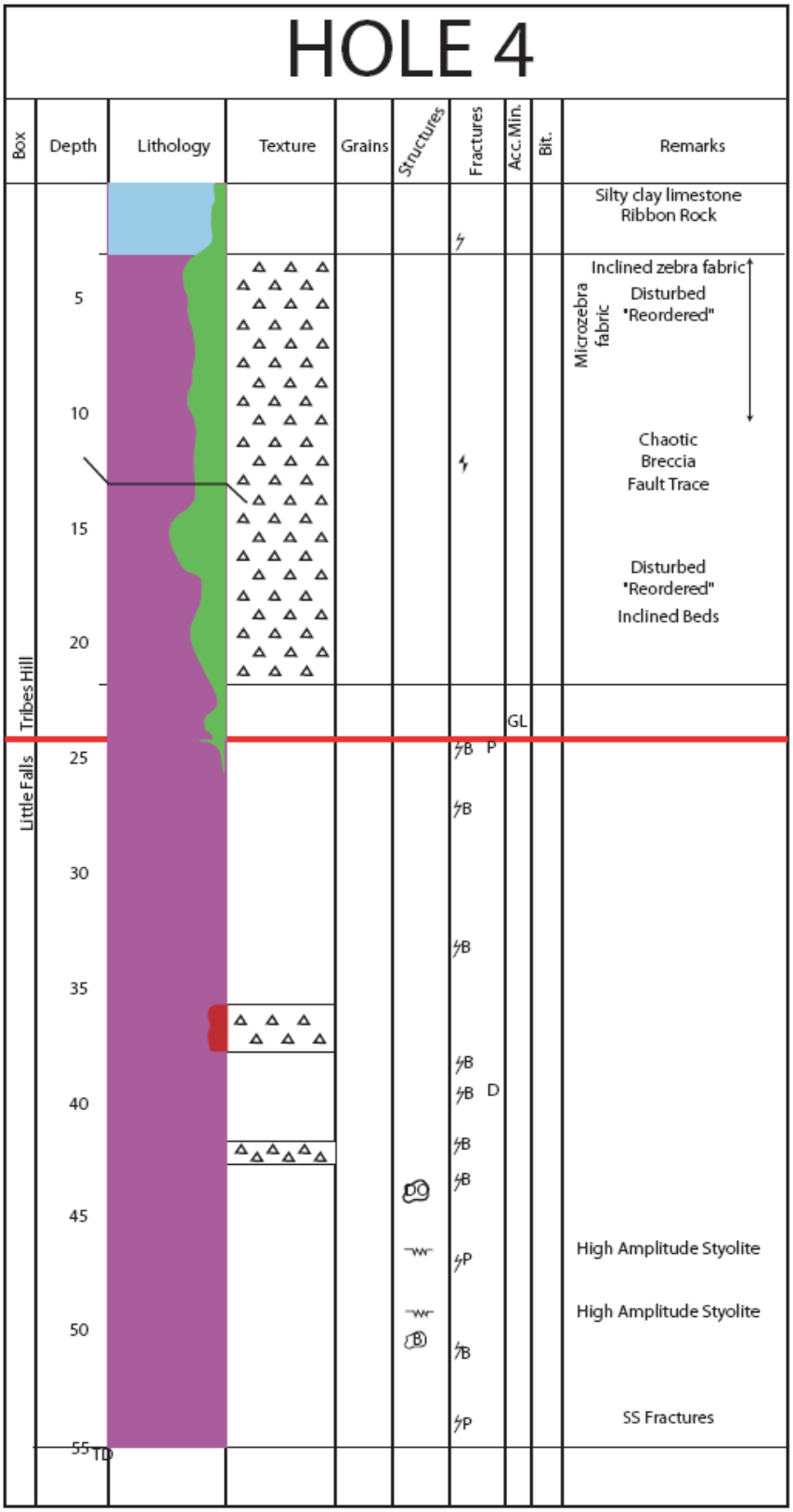

Figure 17 - Hole 4 stratigraphic column with description (digitized from Bray)

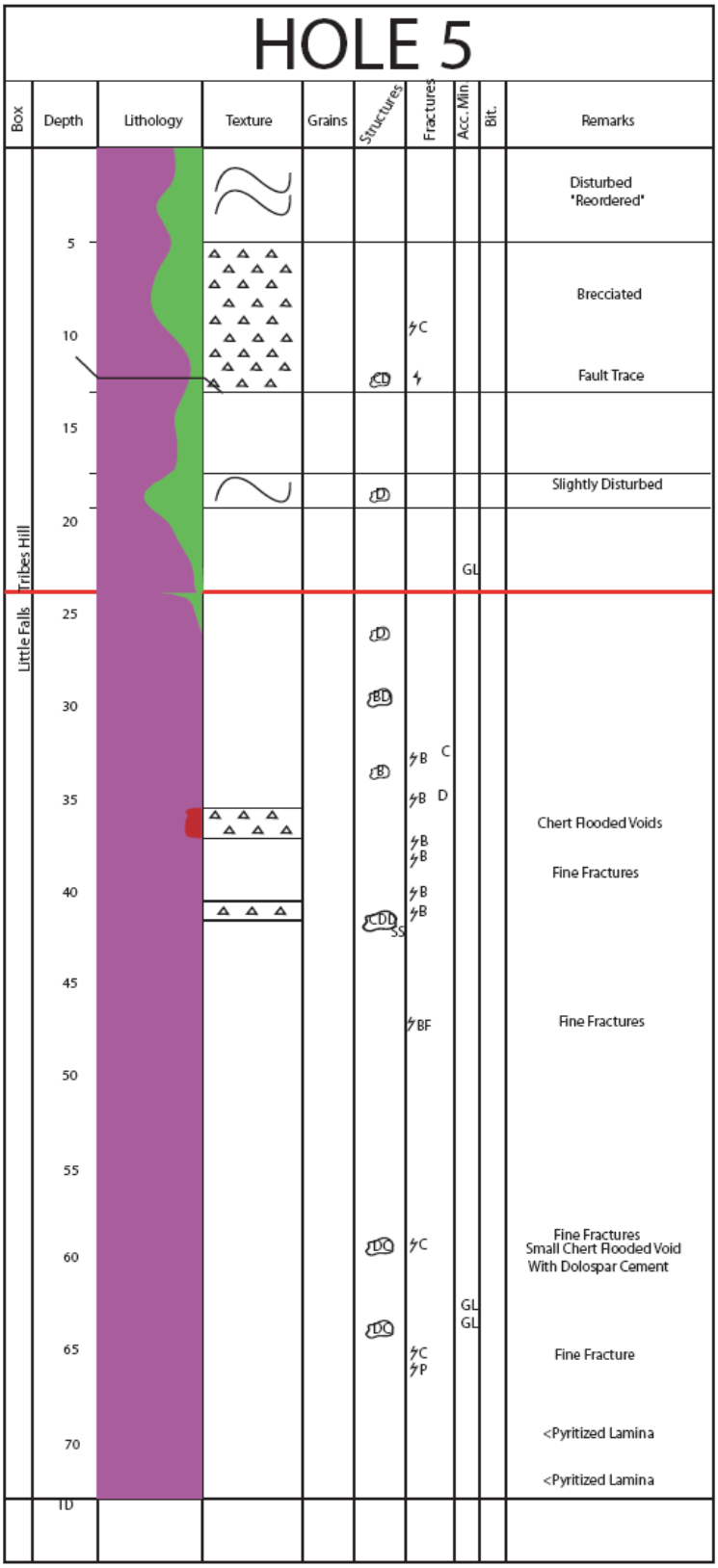

Figure 18 - Hole 5 stratigraphic column with description (digitized from Bray)

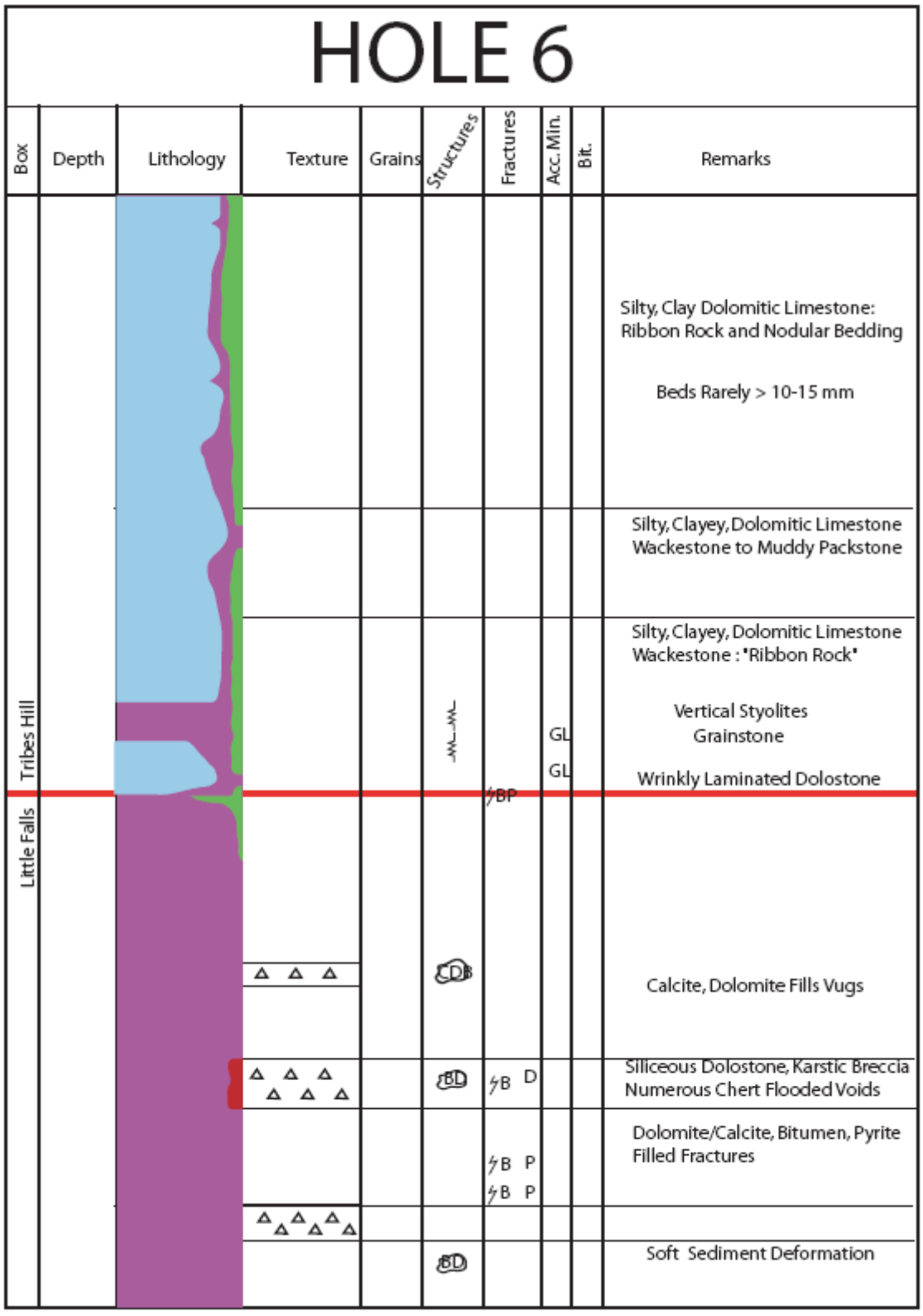

Figure 19 - Hole 6 stratigraphic column with description (digitized from Bray)

Figure 20 shows cross-section 1 which connects Holes 1, 2, and 6. This serves as a stratigraphic profile from the center of the Body 2 (Hole 1) across the fracture zone (Hole 2) and into the unaltered limestone (Hole 6). Hole 1 consists of dolomitized Tribes Hill from the surface to a depth of 24 feet where it reaches the Little Falls contact. Hole 2, located in the fracture zone, approximately five feet north of Hole 1, begins as unaltered limestone, but becomes dolomitized after crossing a fracture at 16 feet Hole 6 was drilled outside of the fractured zone, about 15 feet north of Hole 1, and consists of undolomitized Tribes Hill for the unit's entire thickness, with the exception of a one foot interval of dolostone occurring at a depth of 20 feet.

Figure 21 shows cross-section 2 which connects Holes 1, 3, 4, and 5. Holes 1, 3, and 5 are all located inside the dolomite structure and are, as one would expect, dolomitized throughout their entire length. Hole 4, however, was drilled in the limestone bridge, or gap, between the first and second bodies. The core from this hole reveals that although the bridge is composed of unaltered Tribes Hill at the surface, it crosses a fault and becomes dolomitized only 3 feet. below the quarry floor.

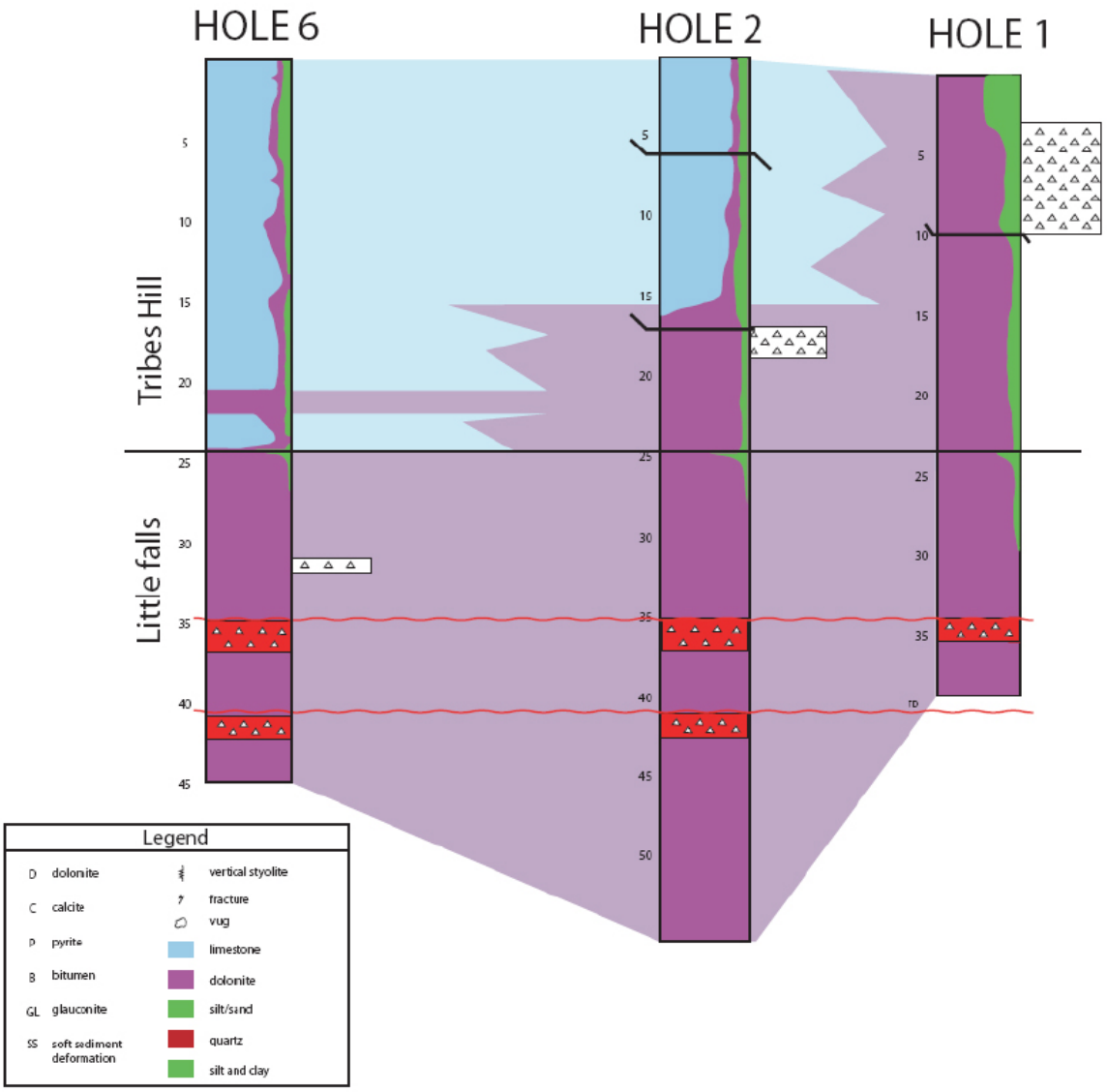

Figure 20 - Cross-section 2, connecting Holes 1, 2, and 6

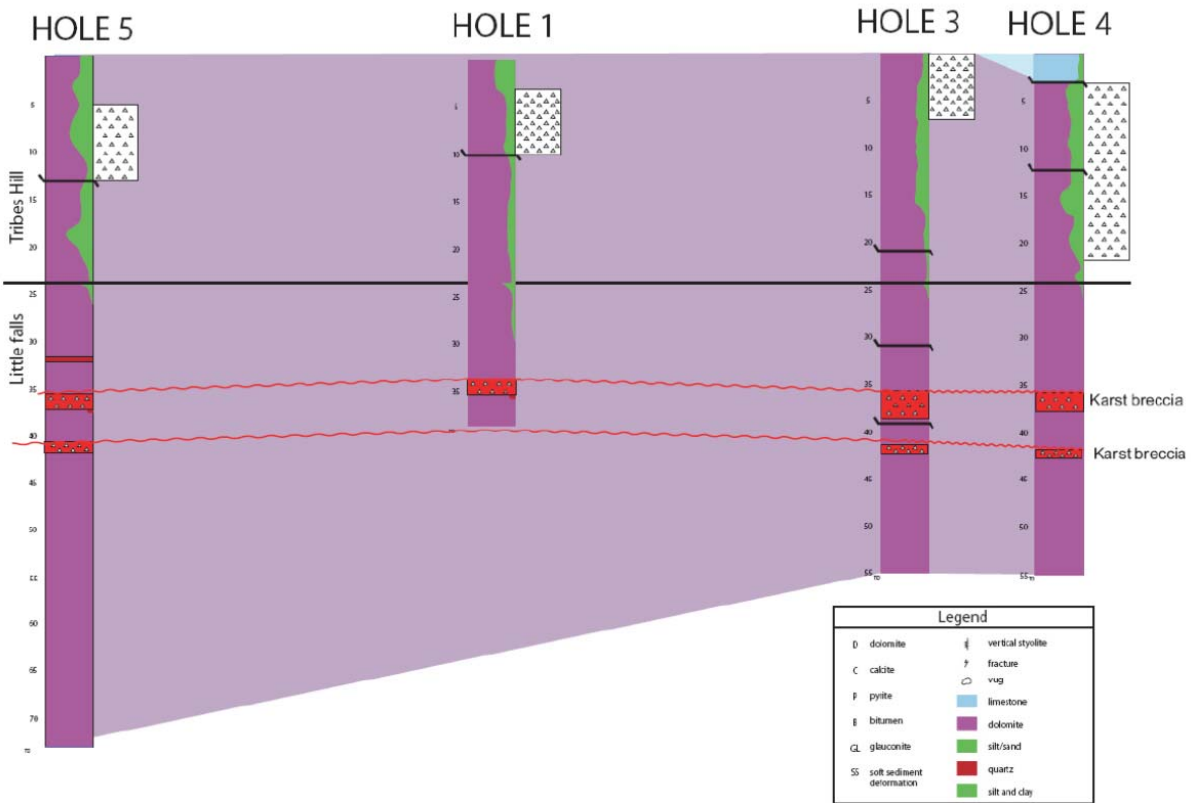

Figure 21 - Cross-section 1, connecting Holes 1, 3, 4, and 5

4.3. Fracture Mapping

Careful examination of the fracture map made in Chapter 3.3 reveals several structures and patterns that may act as clues to determining the orientation of stresses acting on the region during formation of the bodies.

There are calcite veins running from the tips of each body (Fig. 22). These veins range in width from 0.3 to 0.8 inches. The vein associated with the eastern tip of Body 1 runs for roughly 10 feet then bifurcates, forming two smaller veins, which run into a covered interval. Four smaller veins emerge from this covered interval leading to the interpretation that both veins split a second time. These four veins die out within a few

feet of their origin. The western tip/vein of Body 1 and the eastern tip/vein of Body 2 overlap and form the northern and southern boundaries of the bridge (Fig. 23). Both of these veins die out within three to five feet of the bodies.

Figure 22 - Calcite vein running from eastern tip of dolomite body 1

Figure 23 - Aerial view the bridge

Another feature illustrated by the map is the scissor fault that cuts across Body 2 at the jog. This fault begins south east of the jog and runs sub-parallel to the dolomite body dipping to the north. As the fault approaches the jog it bends toward the body and its dip steepens. The fault is nearly vertical as it intersects and cuts through the jog. After exiting the north side of the body the fault bends back to sub-parallel with the body and dips to the south. In this way the fault changes dip as it crosses the dolomite body. Figure 24 shows a series of pictures taken from Trenches 4 and 5 illustrating this change in dip. The significance of the structure is discussed in Chapter 5.4.

The fracture map also shows a relay ramp fault pattern located in the fracture zone along the northern edge of Body 2 (Fig. 25). A relay ramp, as defined by Peacock et al. (2000), is an area of reoriented bedding between two normal faults that overstep in map view and have the same dip direction. The structure begins as a single fault at the eastern tip of Body 2 and runs along the northern edge of the body. It spays to the north at three separate points within 20 feet of the tip, forming separate relay ramps. Note that, as a relay ramp, a single fault block may act as the footwall of one fault and the hanging wall of another.

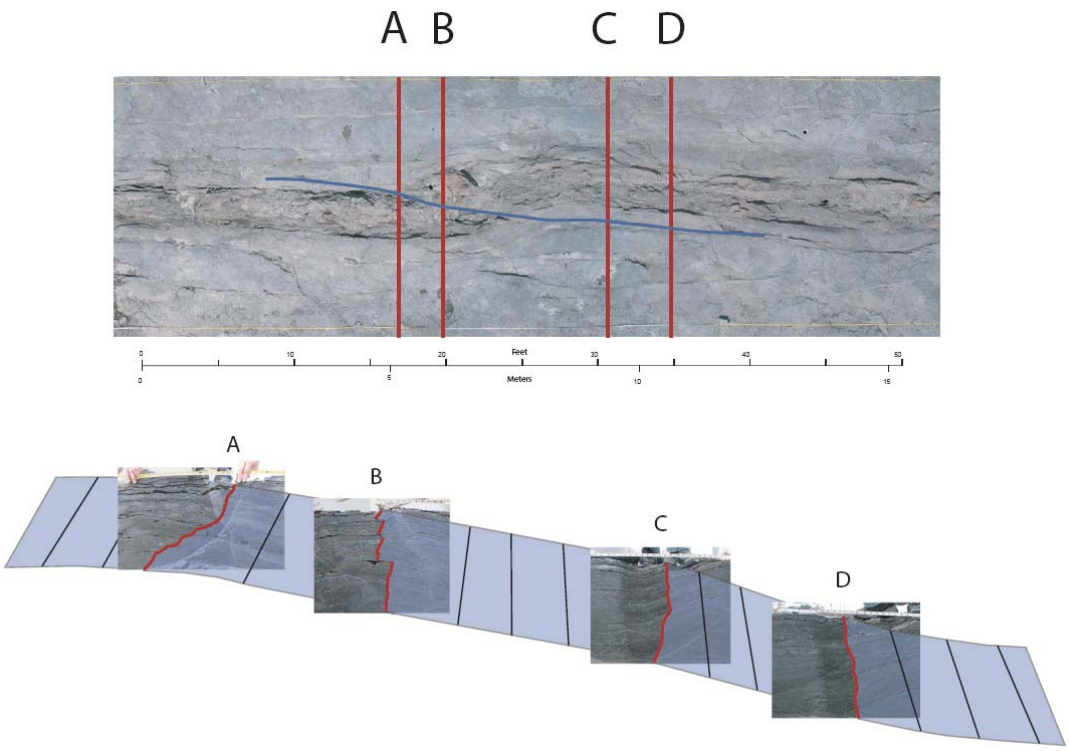

Figure 24 – Illustration of scissor-fault across four trench walls

A) 

B) 

Figure 25 - Relay ramp structure running parallel to the eastern portion of Body 2
A) aerial view B) photo taken from the ground

As mentioned in Chapter 1.4, there are several areas inside the dolomite bodies where brecciation is observed. The most obvious of these occurrences are the tips of each body, however they can also be found in various locations throughout the bodies. Breccia clasts consist of fine grained matrix dolomite surrounded by course grained dolostone (Fig. 26). The locations of all brecciated regions appear on the fracture map. Vugs also occur in many parts of the outcrop. They are commonly found near the brecciated zones at the tips of the bodies. All the vugs are lined with saddle dolomite and calcite. Many also contain quartz and bitumen (Fig. 27). Areas with vuggy porosity are also labeled on the fracture map.

Figure 26 – Cross-section of a brecciated block from inside dolomite body

Figure 27 - A large vug filled with saddle dolomite and calcite crystals, located at the eastern tip of body 1

Another notable structure which appears on the fracture map is the “tail”-like feature connected to the central portion of body two. This long, thin section of coarse grained dolostone extends from the northern side of the jog and runs west, sub-parallel to the western half of the body. It continues for approximately 12 feet then thins to a point. Figure 28 shows an aerial view of the tail, while Figure 29 shows the feature in the wall of trench 5 cuts. From the trench wall, one can see that the “tail” dips to the north away from the dolostone body. The significance of the structure is discussed in Chapter 5.4.

A)

B)

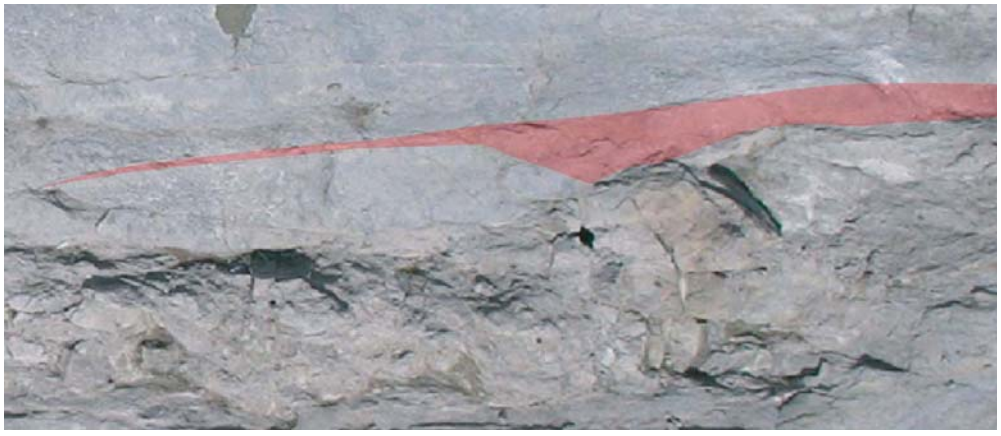

Figure 28 - Aerial photo of the tail-like structure A) without highlight B) with structure highlighted in pink

A) 

B) 

Figure 29 - Profile photos of tail-like structure taken from trench 5 A) looking east B) looking west

4.4. Trenches

Just as the fracture map helped analyze patterns and structures of the outcrop in map view, the walls of the six trenches allow analysis of the bodies and surrounding fracture zone in profile view. Plates 3 through 9 show photo-mosaics made for the walls of each trench.

Variations in color help show the transition from limestone to dolomite. Contact between the limestone and dolomite is gradational, taking place over a distance of approximately six to ten inches (Fig. 30). The texture of the dolostone also coarsens during this transition. Grains of the Tribes Hill Limestone range from 88 to 125μ, while dolostone grains from inside the bodies can measure up to 500μ in diameter.

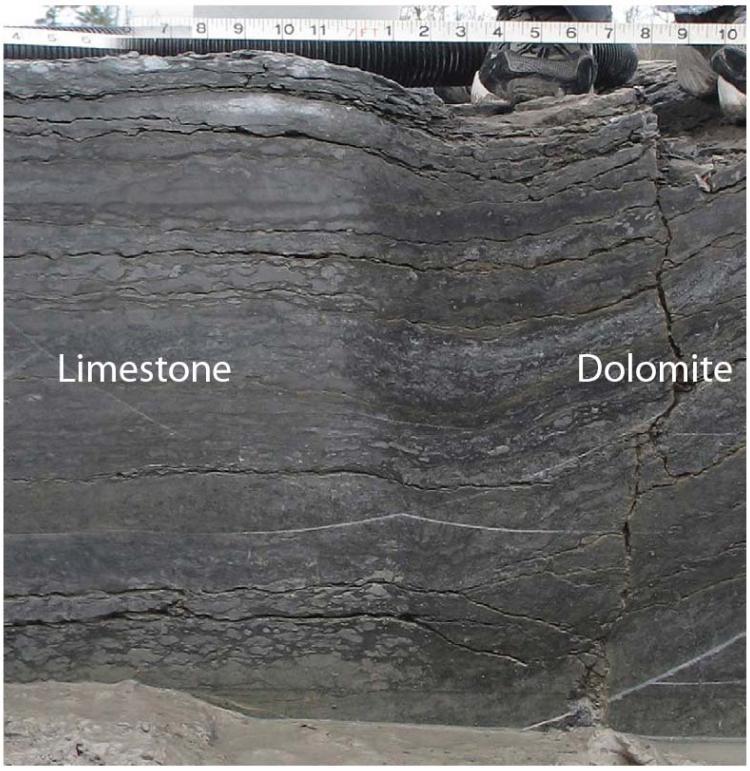

Figure 30 – Transition from limestone to dolomite in Trench 4

Like the GPR profile, the trench walls reveal that both bodies consist of a central syncline, or sag, which is flanked by anticlines on either side. A shaley layer approximately three inches thick appears in a number of the trench walls and serves as a good marker bed for correlation between trenches and for measurement of displacement across fractures/faults. The offset of this bed can be as much as seven inches as seen in Figure 31. Unfortunately, nearly all original rock texture is lost as you enter the dolomitized portion of the trench walls. This makes it impossible to follow an individual layer across the entire body. In each case the central sag consists of a breccia in which clasts have been moved and rotated relative to one another (Fig. 32). This also prevents the measurement of a single layer across the entire width of the outcrop.

Figure 31 - Offset bed in the eastern wall of Trench 5

Figure 32 - Rotated bocks located within the central sag of body 2 (taken from eastern wall of Trench 4)

The trench walls also give excellent exposures of the mineralization along fractures and faults along either side of the bodies. One observation made by looking at the trenches, which could not be seen in map view, is the relationship between amount of mineralization and proximity to the dolomite bodies. The fractures in outer extremes of the fracture zone are fully mineralized with little or no porosity. Moving inward (from either side) toward the transition zone of limestone to dolomite, the fractures become open. Many are lined with saddle dolomite crystals, but void space remains where mineralization has not completely occluded the fractures. Inside the zone of coarse dolomite all fractures are completely open and show no signs of mineralized filling.

Most faults and fractures dip away from the dolostone bodies. However, some change their dip direction as they cross shalier bedding plains, so that where the offset is most visible, the faults actually dip toward the body (Fig. 33). In some cases, movement along faults causes the opening of rhomb-shaped openings. These features have a saddle dolomite lining and calcite fill. Figure 34 shows a rhomb exposed in Trench 6. Figure 35 shows a similar rhomb with slicken-sides indicating the same sense of motion

Figure 33 - Fracture changes dip direction when crossing shaley bed
(taken from eastern wall of Trench 4)

Figure 34 - Rhombohedral pull-apart with red arrow to indicate motion direction
(taken from eastern wall of trench 6)

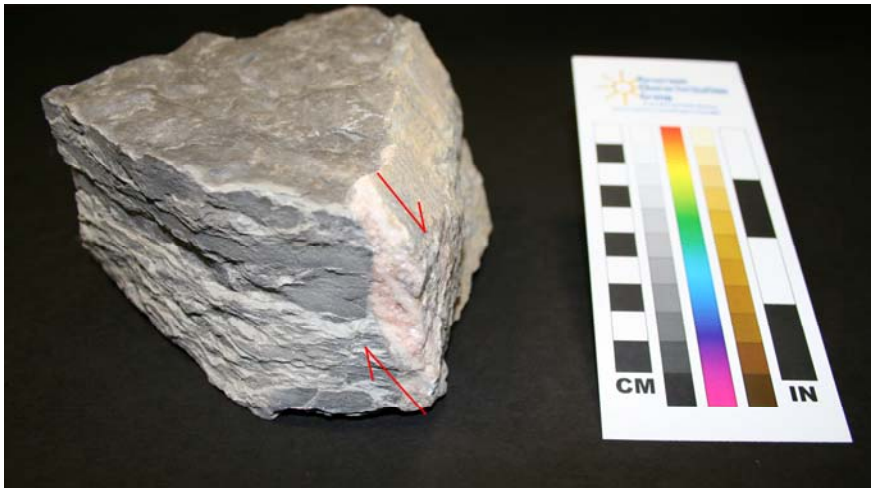

Figure 35 - Calcite/dolomite rhomb with slicken-sides taken from the quarry

4.5. Paragenetic Sequence

Thin sections made from the quarry samples were analyzed at the New York State Museum. These sections helped determine the relative timing of the diagenetic processes that have acted on the Tribes Hill since deposition. Figure 36 is a chart depicting this series of events. Figure 37 shows a thin section example for each event.

The earliest processes to affect the Tribes Hill, fragmentation, desiccation and lithification, are all common in the formation of limestone. Some dolomite replacement occurred before fracturing began and should therefore not be considered hydrothermal. This dolomitization was probably caused by meteoric mixing. The first incidence of fracturing was followed by a second period of dolomite replacement and growth of saddle dolomite crystals. In this case, the dolomitization was directly related to the faulting and can be considered hydrothermal in origin. These saddle crystals are zoned with alternating iron-rich and non iron-rich regions. Later, after continued burial, dedolomitization and dissolution of saddle dolomite occurred. Oil was then emplaced and

dehydrogenated to form bitumen. A second fracturing event caused another episode of hydrothermal fluid flow and precipitation of saddle dolomite, pyrite, and a late calcite spar. The precipitation of Herkimer Diamond type quartz crystals was the last stage in the diagenesis of the Tribes Hill outcrop. These quartz crystals commonly contain solid bitumen inclusions.

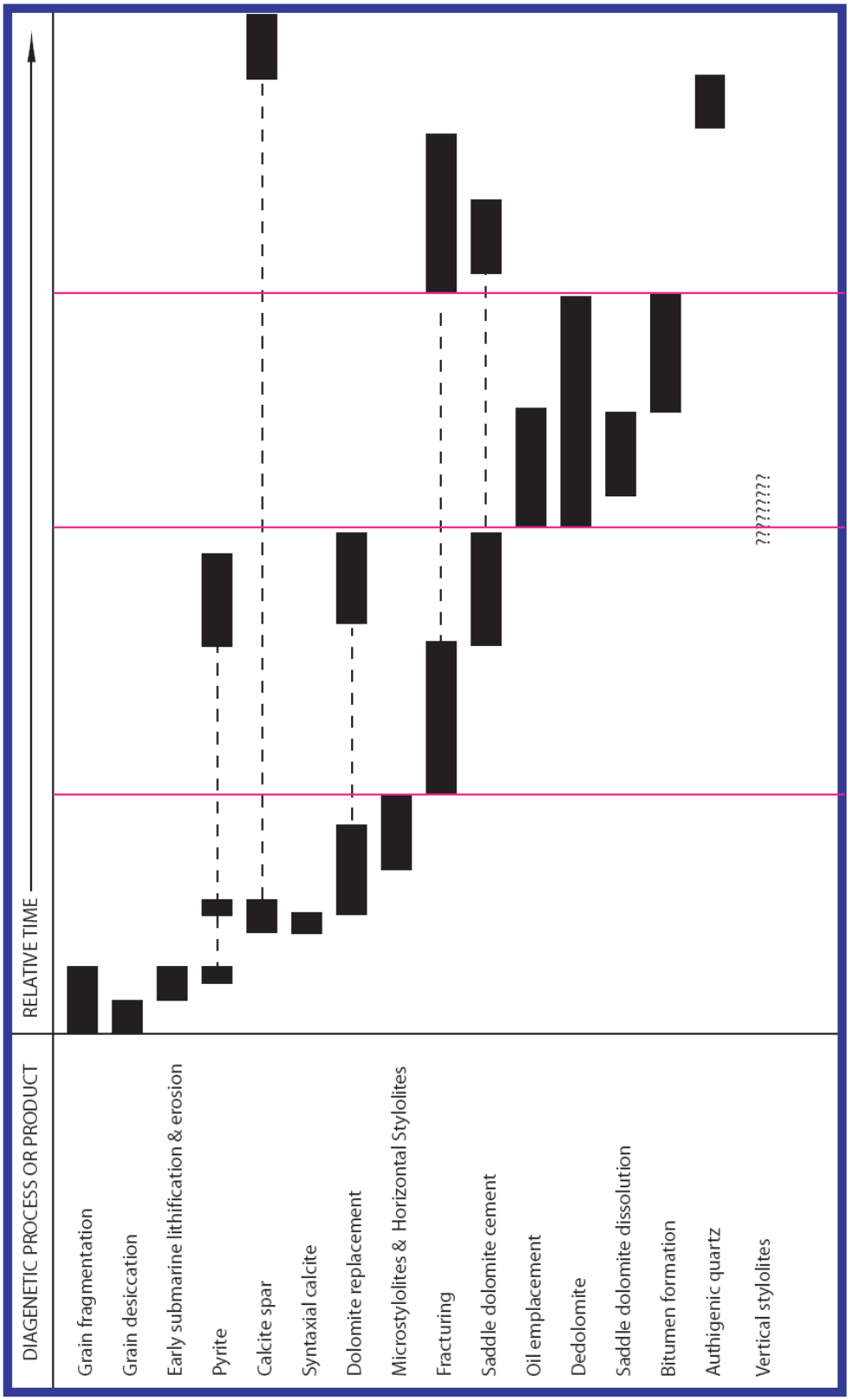

Figure 36 –Graph of paragenetic sequence in relative time

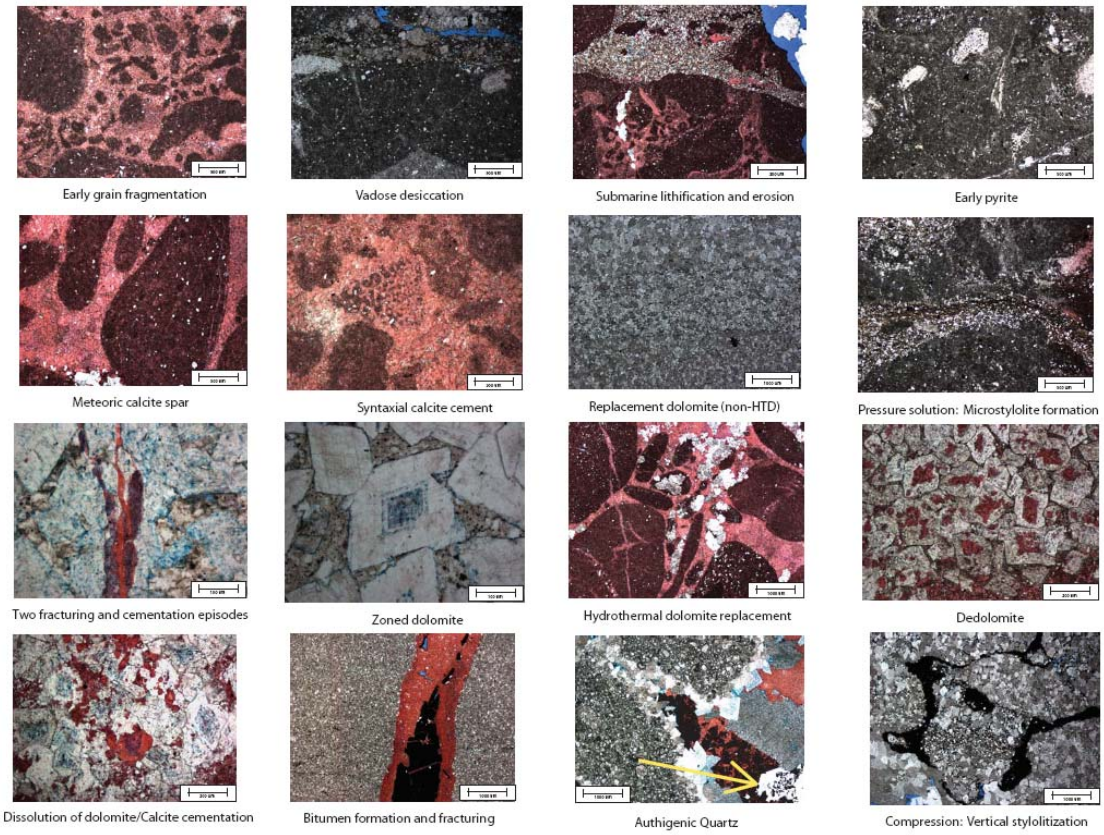

Figure 37 – Thin section images from quarry cores illustrating the types of diagenesis observed

4.6. Stable Isotopes

As described in Chapter 3.6, three sets of samples were tested for $\delta^{13}C$ and $\delta^{18}O$ isotopic ratios. These include the initial surface samples, all plugs from the transect, and the core plugs from Holes 1 and 2. The results of these analyses are shown in Tables 2 through 4 and in Figure 38. Carbon isotope values for dolomite in the Tribes Hill range from -1.31 to -3.06‰ with an average of -2.01‰. Values for the surrounding limestone are slightly more negative with a range of -1.70 to -3.25‰ and an average of -2.19‰. The $\delta^{18}O$ values follow a similar pattern. In the dolostone, values range from -7.66 to -10.74‰ with an average of -8.86‰, while in the limestone ratios range from -8.52 to -11.40‰ and have an average of -9.49‰. It should be noted here that all the $\delta^{18}O$ values for both limestone and dolostone in the quarry are more negative than marine dolomites which typically have values between +1 and +5‰ and/or evaporitic dolomites which range from -1 to +8‰ (Warren, J., 2000).

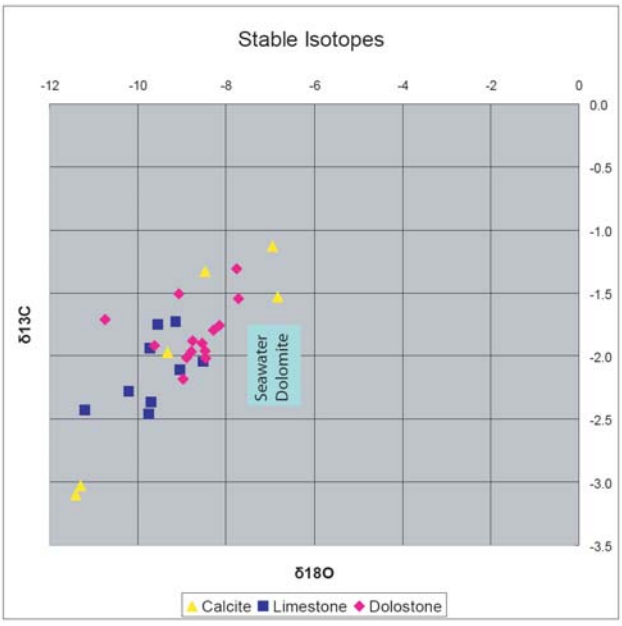

Figure 38 - Cross-plot of stable isotope ratios in comparison with the standard seawater dolomite window

Table II - Stable isotope results for transect plugs

ID #	Footage	Sampled	Comments	SI δ18O	SI δ13C
T1-1	1	transect plugs	outside fracture zone-limestone	-9.01	-1.86
T1-2	2	transect plugs	outside fracture zone-limestone	-9.20	-2.07
T1-3	3	transect plugs	outside fracture zone-limestone	-9.06	-2.07
T1-4	4	transect plugs	outside fracture zone-limestone	-8.79	-1.78
T1-5	5	transect plugs	outside fracture zone-limestone	-10.49	-3.25
T1-6	6	transect plugs	outside fracture zone-limestone	-9.86	-1.85
T1-7	7	transect plugs	outside fracture zone-limestone	-9.55	-2.17
T1-8	8	transect plugs	outside fracture zone-limestone	-9.76	-2.29
T1-9	9	transect plugs	outside fracture zone-limestone	-9.16	-2.09
T1-10	10	transect plugs	outside fracture zone-limestone	-9.14	-2.53
T1-11	11	transect plugs	outside fracture zone-limestone	-9.48	-2.25
T1-12	12	transect plugs	outside fracture zone-limestone	-9.15	-1.98
T1-13	13	transect plugs	outside fracture zone-limestone	-9.53	-2.16
T1-14	14	transect plugs	outside fracture zone-limestone	-9.76	-2.96
T1-15	15	transect plugs	outside fracture zone-limestone	-8.62	-1.70
T1-16	16	transect plugs	outside fracture zone-limestone	-9.69	-2.25
T1-17	17	transect plugs	outside fracture zone-limestone	-10.45	-2.50
T1-18	18	transect plugs	outside fracture zone-limestone	-9.38	-2.13
T1-19	19	transect plugs	outside fracture zone-limestone	-8.54	-1.81
T1-20	20	transect plugs	outside fracture zone-limestone	-10.11	-2.27
T1-21	21	transect plugs	outside fracture zone-limestone	-9.44	-3.10
T1-22	22	transect plugs	outside fracture zone-limestone	-9.61	-2.22
T1-23	23	transect plugs	outside fracture zone-limestone	-8.90	-1.81
T1-24	24	transect plugs	outside fracture zone-limestone	-8.81	-1.99
T1-25	25	transect plugs	first fracture- fades into dolostone	-11.40	-2.87
T1-25.5	25.5	transect plugs	inside fracture zone	-9.54	-2.18
T1-26	26	transect plugs	inside fracture zone	-10.00	-2.17
T1-26.5D	26.5	transect plugs	inside fracture zone	-9.31	-2.48
T1-26.5L	26.5	transect plugs	inside fracture zone	-8.82	-1.87
T1-27	27	transect plugs	inside fracture zone	-9.02	-2.10
T1-27.5	27.5	transect plugs	inside fracture zone	-9.53	-2.29
T1-28	28	transect plugs	inside fracture zone	-7.88	-1.38
T1-29.5	29.5	transect plugs	inside fracture zone	-8.73	-2.02
T1-30	30	transect plugs	inside fracture zone	-8.62	-2.51
T1-30.5	30.5	transect plugs	inside fracture zone	-8.72	-1.73
T1-31	31	transect plugs	inside fracture zone	-8.34	-1.86
T1-31.5	31.5	transect plugs	inside fracture zone	-8.92	-1.95
T1-32	32	transect plugs	inside fracture zone	-8.30	-1.64
T1-33	33	transect plugs	inside fracture zone	-8.30	-2.01
T1-33.5	33.5	transect plugs	inside fracture zone	-8.90	-3.06
T1-34	34	transect plugs	inside fracture zone	-8.91	-2.52
T1-34.5	34.5	transect plugs	inside fracture zone	-8.30	-1.47
T1-35	35	transect plugs	inside fracture zone	-8.75	-2.60
T1-35.5	35.5	transect plugs	inside fracture zone	-10.06	-2.75
T1-36	36	transect plugs	inside fracture zone	-9.83	-2.19
T1-36.5	36.5	transect plugs	last fracture- fades out of dolostone	-9.43	-2.12
T1-38	38	transect plugs	outside fracture zone-limestone	-9.52	-2.13
T1-39	39	transect plugs	outside fracture zone-limestone	-9.03	-2.12
T1-41	41	transect plugs	outside fracture zone-limestone	-9.05	-1.92

Table III - Stable isotope results for core plugs

ID #	Footage	Sampled	Comments	SI $\delta^{18}O$	SI $\delta^{13}C$
H1D3	3	plugs from cores	limestone	-9.44	-1.88
H1D5	5	plugs from cores	dolostone	-10.38	-2.24
H1D7	7	plugs from cores	dolostone	-8.78	-2.10
H1D9	9	plugs from cores	dolostone	-8.35	-1.99
H1D11	11	plugs from cores	dolostone	-8.58	-1.68
H1D13	13	plugs from cores	dolostone	-7.66	-2.01
H1D15	15	plugs from cores	dolostone	-8.97	-2.18
H1D17	17	plugs from cores	dolostone	-8.16	-1.76
H1D19	19	plugs from cores	dolostone	-8.29	-1.79
H1D21	21	plugs from cores	dolostone	-7.72	-1.54
H1D27	27	plugs from cores	LF dolostone	-5.75	-1.45
H1D29	29	plugs from cores	LF dolostone	-8.81	-2.12
H1D31	31	plugs from cores	LF dolostone	-6.98	-1.31
H1D33	33	plugs from cores	LF dolostone	-8.48	-2.26
H1D35	35	plugs from cores	LF dolostone	-5.51	-1.08
H2D1.5	1.5	plugs from cores	Limestone	-10.20	-2.28
H2D3m	3	plugs from cores	LS matrix	-9.72	-1.94
H2D5.7d	5.7	plugs from cores	dolomite	-10.74	-1.71
H2D7.2m	7.2	plugs from cores	dolostone matrix	-9.63	-1.92
H2D9	9	plugs from cores	Limestone	-9.14	-1.73
H2D11	11	plugs from cores	Limestone	-9.54	-1.75
H2D13	13	plugs from cores	Limestone	-11.21	-2.43
H2D19	19	plugs from cores	Dolostone	-7.76	-1.31
H2D23	23	plugs from cores	Dolostone	-8.76	-1.88
H2D25	25	plugs from cores	LF Dolostone	-7.31	-1.74
H2D27	27	plugs from cores	LF Dolostone	-8.13	-1.96
H2D29c	29	plugs from cores	calcite	-6.83	-1.53
H2D29m	29	plugs from cores	LF dolostone matrix	-7.27	-1.52
H2D31c	31	plugs from cores	calcite	-6.95	-1.13
H2D33	33	plugs from cores	LF dolostone	-7.51	-1.86
H2D35	35	plugs from cores	LF dolostone	-6.93	-2.14
H2D37	37	plugs from cores	LF dolostone	-4.90	-1.07

Table IV - Stable isotope results for surface samples

ID #	Sampled	Comments	SI $\delta^{18}O$	SI $\delta^{13}C$
PB1	Up against fault	Dolostone matrix	-8.47	-2.02
PB2	Up against fault	Dolostone matrix	-8.47	-1.96
PB3	Up against fault	Dolostone matrix	-8.55	-1.90
PB5	6" from dolomite	Limestone matrix	-9.04	-2.11
PB6	3' from fault	Limestone matrix	-9.70	-2.37
PB7c	fault Related	Calcite	-8.48	-1.33
PB7d	fault Related	Dolostone matrix	-9.07	-1.51
PB8c	Fault Related	Calcite	-11.41	-3.10
PB9	Fault Related	Limestone matrix	-8.52	-2.05
PB10	Fault Related	Dolostone matrix	-8.79	-1.97
PB11c	Fault Related	Calcite	-11.30	-3.03
PB11L	Fault Related	Limestone matrix	-9.75	-2.46
PB13	Fault Related	Calcite	-9.33	-1.97
PB14	dolomite from fault	Dolostone matrix	-8.90	-2.01

Strontium isotope analyses were run on the first set of samples collected. This set includes seven samples of dolostone, four of the Tribes Hill limestone, and four of vein filling calcite from the fracture zone. The results of these tests are reported in Table 5 and shown in Figure 39. The dolostone values ranged from 0.7090 to 0.7103 with an average of 0.7098 and a standard deviation of 4.21×10^{-4}. The 0.7090 value appears to be an outlier from the rest of the data as it is drastically different than any of the other samples. The limestone values are a bit lower those of the dolostone. They range from 0.7091 to 0.7094 with an average of 0.7093 and a standard deviation of 1.25×10^{-4}. The $^{87}Sr/^{86}Sr$ tests on the calcites yield values still lower, with the exception of one outlier. They have a range of 0.7091 to 0.7116 with an average of 0.7099 and a standard deviation of 1.28×10^{-3}. The inferences made and conclusions derived from this data are given in the discussion, Chapter 5.

Table V - Strontium isotope results for surface samples

ID #	Sampled	Comments	Sr
PB1	Up against fault	Dolostone matrix	0.7095362
PB2	Up against fault	Dolostone matrix	0.7097077
PB3	Up against fault	Dolostone matrix	0.7101632
PB4	Fault Related	Dolostone matrix	0.7102665
PB5	6" from dolomite	Limestone matrix	0.70909
PB6	3' from fault	Limestone matrix	0.7093616
PB7c	fault Related	Calcite	0.7115766
PB7d	fault Related	Dolostone matrix	0.7103485
PB8c	Fault Related	Calcite	0.708903
PB9	Fault Related	Limestone matrix	0.7093411
PB10	Fault Related	Dolostone matrix	0.7098332
PB11c	Fault Related	Calcite	0.7090517
PB11L	Fault Related	Limestone matrix	0.709223
PB13	Fault Related	Calcite	0.7091137
PB14	dolomite from fault	Dolostone matrix	0.7096135

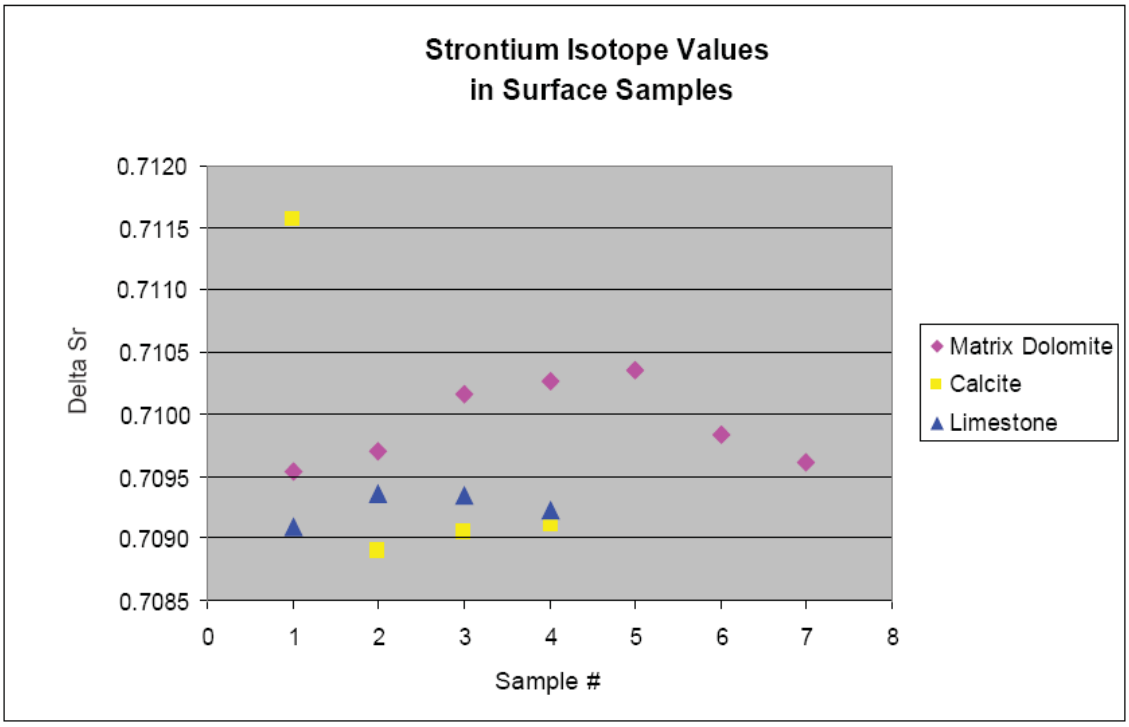

Figure 39 - Graph of strontium isotope values from surface samples collected in the quarry

4.7. Fluid Inclusions

As discussed in Chapter 3.7, fluid inclusion analyses were performed in two separate batches. One set, consisting of two samples, was sent to Fluid Inclusion Technologies Inc. (FIT) for testing, while a second set of ten were analyzed at the University of Albany.

The two samples sent to FIT were given the names PB200 and PB201. A summary of their results follows and FIT's full results are available in Appendix 2. Table 6 contains the data from their analyses. Sample PB200 was made up of a coarse matrix dolomite, a very coarse saddle dolospar and late calcite. Primary inclusions in the matrix dolomite range from 120-130°C and intermediate salinities. Secondary or pseudo-

secondary inclusions in the early calcite are 80-95°C with salinities of 26-28 wt.% salt, while secondary or pseudo-secondary inclusions in the late calcite cement have homogenization temperatures of 65-75°C and salinities of 14.5-18.6 wt.%. Sample PB201 consisted of mainly coarse zoned dolomite with some late calcspar. Primary aqueous inclusions in the dolomite have homogenization temperatures of 105-132°C and secondary or pseudo-secondary inclusions had homogenization temperatures of 90-129°C. Salinities ranged from 26-30 wt.% NaCl (near halite saturation).

Table VI- Fluid inclusion results from samples sent to FIT

FIT Samples	Population	Type	Th °C	Tm °C	Sal (wt%)
PB 200	late calcite A	s / ps	65 - 75	-13.0 to -14.0	16.9 - 17.8
PB 200	late calcite B	s / ps	65 - 75	-13.5 to -14.5	17.3 - 18.2
PB 200	late calcite C	s / ps	65 - 75	-14.0 to -15.0	17.8 - 18.6
PB 200	late calcite D	s / ps	120 - 130	10.5 to -11.0	14.5 - 15.0
PB 200	matrix calcite E	s / ps	80 - 95	-30 to -35	26 - 28
PB 200	matrix dol F	pr / s	120 - 130	-	-
PB 200	matrix dol G	pr / s	120 - 130	-	-
PB 201	dol core A	pr / ps	95 - 105	-30 to -40	26 - 30
PB 201	dol mid A	pr / s	100 - 110	-30 to -40	26 - 30
PB 201	dol mid A	pr / s	90 - 100	-30 to -40	26 - 30
PB 201	dol rim A	pr / s	90 - 95	-30 to -40	26 - 30
PB 201	dol rim B	pr / s	95 - 105	-30 to -40	26 - 30
PB 201	dol rim C	pr	110 - 120	-30 to -40	26 - 30
PB 201	dol mid D	pr / s	110 - 120	-30 to -40	26 - 30
PB 201	dol mid D	pr / s	120 - 125	-30 to -40	26 - 30
PB 201	dol rim E	pr	132	-30 to -40	26 - 30
PB 201	dol core F	pr / s	129	-30 to -40	26 - 30
PB 201	dol outer core G	pr	105 - 115	-40.0	30.0
PB 201	dol rim H	pr	120 - 130	-30 to -35	26 - 28
PB 201	dol rim I	pr	125 - 130	-30 to -35	26 - 28

The second set of inclusions, analyzed at the University of Albany, support and supplement the data from FIT. All the inclusions analyzed were determined to be primary or pseudo-secondary based on the criteria set forth by Goldstein and Reynolds (1994). Inclusions which were confined to growth zones were labeled primary, while inclusions with seemingly random distribution, no association with secondary features, and no clear association with growth zonation were labeled pseudo-secondary. Unfortunately, all 41 of the inclusions found were extremely small, less than 3μm, and were not frozen since the ice would be too difficult observe. Therefore, no melt temperatures or subsequent salinities were obtained from these analyses. Vapor bubbles were clearly visible in every inclusion and homogenization temperatures were measured to the nearest 1.0°C. These homogenization temperatures are reported in Table 7 and plotted graphically in Fig 40. The inclusions found in saddle dolomite crystals yielded the highest homogenization temperatures, ranging from 132 - 154°C with an average of 139°C. Matrix dolomite inclusions were slightly cooler with a range of 107 - 135°C and an average of 121°C. The calcite inclusions were also cooler than the saddle crystals. They ranged from 104 - 132°C with an average of 117°C. Interpretations of this data are discussed in Chapter 5.2.

Table VII - Fluid inclusion results from samples analyzed at SUNY Albany

Sample ID	Source	Type	Th °C
SB1-1 (surface body 1)	matrix dolomite	pr / ps	120
SB1-2 (surface body 1)	matrix dolomite	pr / ps	135
SB1-3 (surface body 1)	matrix dolomite	primary	119
SB2-1 (surface body 2)	matrix dolomite	pr / ps	111
SB2-2 (surface body 2)	matrix dolomite	primary	124
SB2-3 (surface body 2)	matrix dolomite	pr / ps	112
SB2-4 (surface body 2)	matrix dolomite	pr / ps	109
FF1-1 (fracture fill 1)	calcite	pr / ps	129
FF1-2 (fracture fill 1)	calcite	pr / ps	119
FF1-3 (fracture fill 1)	calcite	pr / ps	132
FF2-1 (fracture fill 2)	calcite	pr / ps	106
FF2-2 (fracture fill 2)	calcite	pr / ps	122
FF2-3 (fracture fill 2)	calcite	pr / ps	108
FF2-4 (fracture fill 2)	calcite	pr / ps	104
FF2-5 (fracture fill 2)	calcite	pr / ps	113
FF3-1 (fracture fill 3)	calcite	pr / ps	119
P1-1 (plug 1)	matrix dolomite	pr / ps	120
P1-2 (plug 1)	matrix dolomite	pr / ps	113
P1-3 (plug 1)	matrix dolomite	pr / ps	126
P1-4 (plug 1)	matrix dolomite	pr / ps	119
P2-1 (plug 2)	matrix dolomite	pr / ps	123
P2-2 (plug 2)	matrix dolomite	pr / ps	118
P2-3 (plug 2)	matrix dolomite	pr / ps	113
P2-4 (plug 2)	matrix dolomite	pr / ps	107
P3-1 (plug 3)	matrix dolomite	pr / ps	128
P3-2 (plug 3)	matrix dolomite	pr / ps	139
P3-3 (plug 3)	matrix dolomite	pr / ps	132
P3-4 (plug 3)	matrix dolomite	pr / ps	127
P3-5 (plug 3)	matrix dolomite	pr / ps	133
VF1-1 (vug fill 1)	saddle dolomite	primary	141
VF1-2 (vug fill 1)	saddle dolomite	primary	137
VF1-3 (vug fill 1)	saddle dolomite	primary	137
VF1-4 (vug fill 1)	saddle dolomite	primary	140
VF2-1 (vug fill 1)	saddle dolomite	pr / ps	136
VF2-2 (vug fill 2)	saddle dolomite	pr / ps	132
VF2-3 (vug fill 2)	saddle dolomite	pr / ps	132
VF2-4 (vug fill 2)	saddle dolomite	pr / ps	134
VF2-5 (vug fill 2)	saddle dolomite	pr / ps	142
VF2-6 (vug fill 2)	saddle dolomite	pr / ps	148
VF2-7 (vug fill 2)	saddle dolomite	pr / ps	154

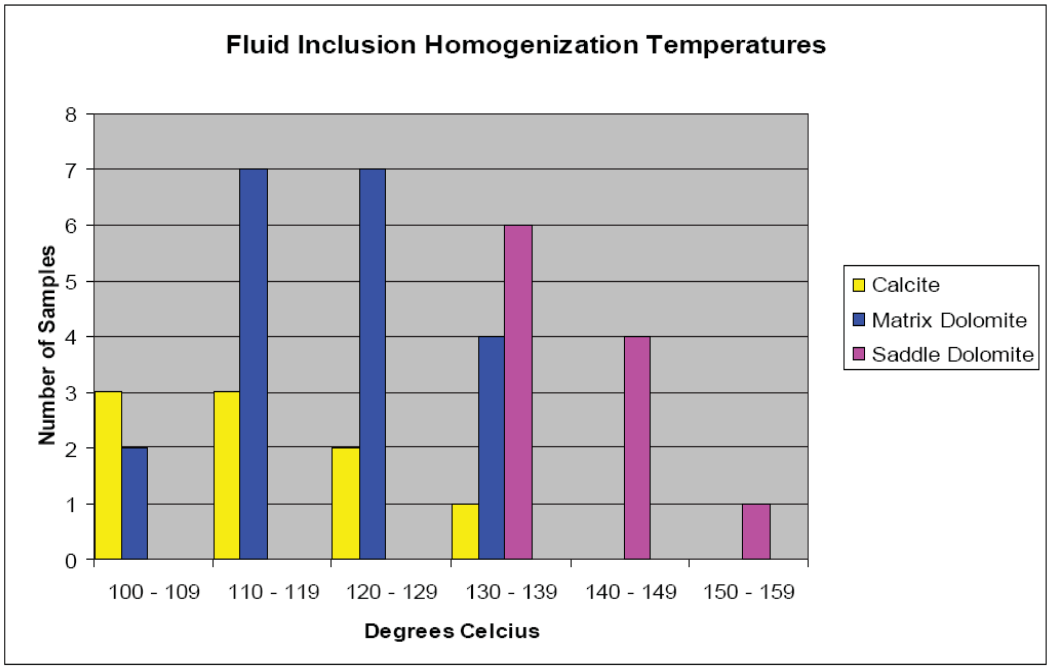

Figure 40 - Graph of homogenization temperatures from fluid inclusions analyzed at SUNY Albany

Chapter 5 – Discussion

5.1. Hydrothermal Alteration in Palatine Bridge

Although there is no single characteristic of the Palatine Bridge outcrop that can unequivocally prove its origin to be hydrothermal, the compilation of data from geochemical, structural, and pertrographical analyses make a strong argument for dolomitization by means of relatively hot fluids which have traveled from depth by way of fault and fracture flow paths.

The most obvious indications of fault control on dolomitization in the quarry are field relations and geometry of the outcrop. Other near surface processes of dolomitization should all produce a widespread, laterally extensive dolomite. The quarry dolomite only occurs around mineralized faults and fractures and is absent away from the faults. Fluid flow along fault planes is also evident in the cores. Figure 41 is an image of core taken from Hole 2 at a depth of 31 feet. Calcite mineralization along the fracture gives good evidence for the passage of fluids and precipitation of minerals along openings in the Little Falls and upward into the Tribes Hill. The dolomitized breccias present at the tips and within the dolomite bodies suggests fault control on brecciation as well as dolomitization. This texture has been interpreted as a fault breccia and is related to the lengthwise propagation of the bodies as they developed.

Despite its clear association with faulting, there are other processes of dolomitization that cannot be completely discounted by the geometry of the outcrop alone. For example, localized dolomite formations have also been interpreted to form in karst environments (Loucks, 1998). These structures may also contain breccias, however

they are related to cave collapse rather than faulting. Field relations alone are not enough to scientifically eliminate this process as a possible origin of the outcrop. Therefore geochemical and fluid inclusion analyses are required.

Figure 41 - Calcite mineralization in a fracture from Hole 2 core at 31 ft.

Homogenization temperatures (T_H) measured in primary aqueous inclusions give the minimum temperature of the parent fluid from which a given crystal was precipitated. Therefore, by comparing the Homogenization temperatures of a hydrothermal formation to the maximum burial temperature of the unaltered host rock, one may see that the fluids were hotter than the host rock had ever been. Such is the case for many hydrothermal dolomite gas fields (Allan & Wiggins, 1993; Smith, 2006). Although finding homogenization temperatures greater than a unit's maximum burial temperature is an excellent way to prove hydrothermal alteration, it should be noted that homogenization temperatures lower than the maximum burial temperature do not conclusively prove that a structure is not hydrothermal in origin. A unit may be altered at a shallow depth, when the fluids traveling upward along fault planes are hotter than the surrounding rock. Then subsequent burial may expose the unit to temperatures greater than that of the fluid. Homogenization temperatures from the unit would not be hotter than the unit's maximum burial temperature, yet it did undergo hydrothermal alteration.

Unfortunately, the homogenization temperatures from the quarry sample inclusions do not conclusively prove that the dolomite formed by hydrothermal alteration. Conodont alteration studies performed in upstate New York yield CAI values of 3.5 in Ordovician aged rocks of the Mohawk Valley (Weary et al., 2001). Using the equations established by Hulver (1997) this translates to a burial temperature between 142°C and 206°C. Therefore, the homogenization temperatures from the quarry inclusions (107-154°C) may fall above or below the actual maximum burial temperature for the Tribes Hill.

By plotting the $^{87}Sr/^{86}Sr$ values for the quarry samples in reference to that of seawater (Fig. 42) it is clear that the unaltered Tribes Hill limestone samples lie directly on the seawater curve for the early Ordovician, the time of their deposition. The dolomite samples, however, plot above the seawater curve, indicating that they did not precipitate from the same marine fluids. In fact, the dolomites plot above all values for the seawater curve interpretation. This enrichment of the dolomite in radiogenic strontium can be attributed to interaction between the parent fluid and the metamorphic rocks of the Precambrian Basement. Therefore, these fluids must have circulated through the basement or overlying immature silici-clastics prior to precipitating dolomite.

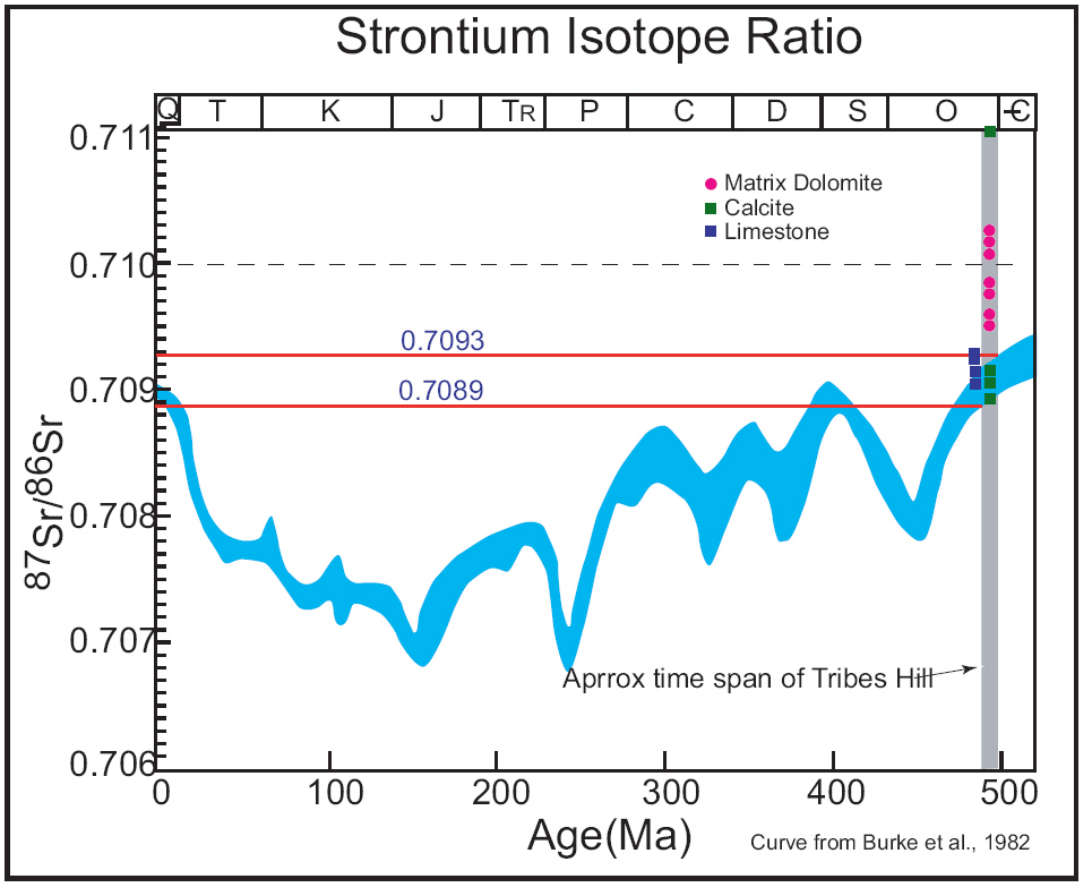

Figure 42 - Strontium isotope ratios from quarry samples plotted in comparison with that of prehistoric seawater

As noted in chapter 4.6, the oxygen isotope values for the quarry dolomites are about two parts per mil lighter than normal seawater dolomite. However, the temperature of the parent fluid must be considered when working out its original composition. Figure 43 shows a temperature vs. $\delta^{18}O$ cross plot of matrix dolomite from the quarry. These samples plot in the range of +2‰ while Late Ordovician seawater has been calculated to have been approximately -6‰ (Smith, 2006).

Where salinities were able to be measured, the fluid inclusions had 26-30 wt% NaCl. These values are much higher than seawater salinity, in fact they boarder on halite saturation (31-32 wt%). When combined with the strontium and stable isotope data it becomes clear that dolomitization of the quarry outcrop took place under the influence of fluids which were geochemically disparate from normal ocean water.

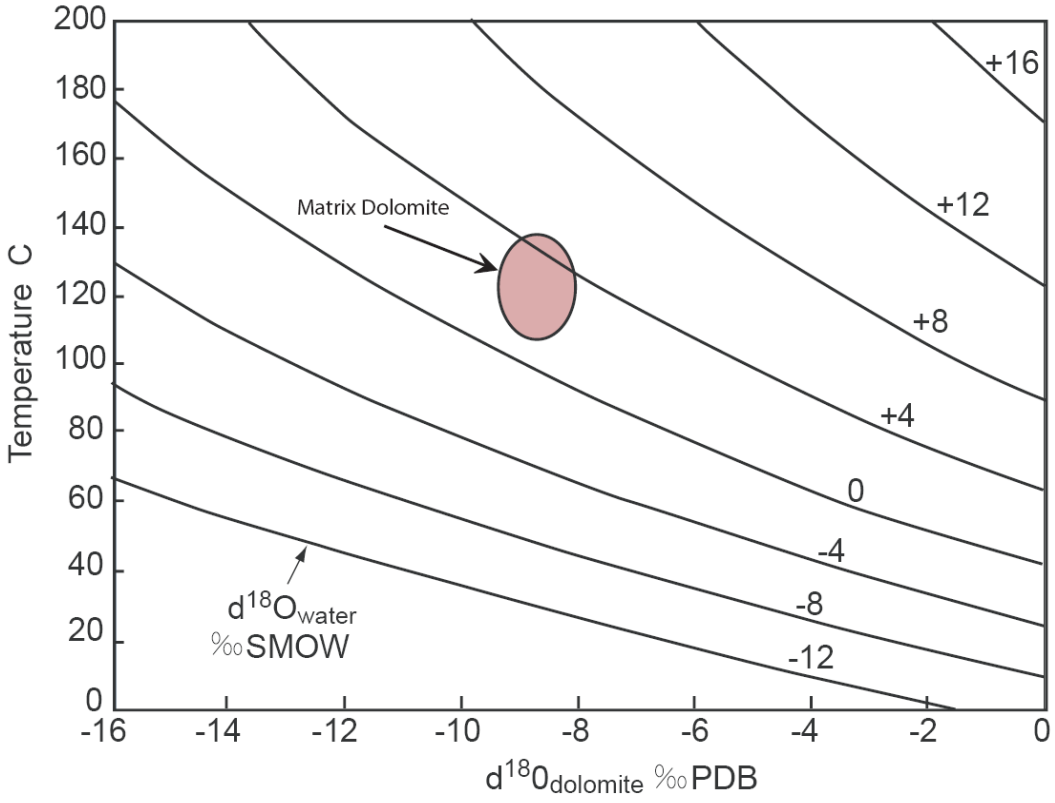

Figure 43 – Homogenization temperature vs. $\delta^{18}O$ cross plot

5.2. Timing of Faulting and Fluid Flow

Because the formation of hydrothermal dolomite is reliant on the release of pressurized fluids trapped at depth, faulting and fracturing are necessary components of the process (Davies and Smith, 2006). It is important to note that formation of the dolomite bodies is unlikely to have occurred in a single event, but rather throughout a sequence of fluid flow episodes. It is equally important to note that mineralization is most likely to occur while faults are active, not after.

Geochemical analysis of dolomite crystals from around the world have shown that the crystals are typically zoned, like those found in the Palatine Bridge Quarry (Fig. 44) (Braithwaite, 1997; Auajjar et al., 2002). Two hypotheses have been suggested to explain this occurrence. 1. The chemical composition of the fluid may have changed during crystallization while fluid flow itself remained continuous. But more likely, 2. the crystal grew episodically with a series of short fluid flow events each with a slightly different chemical composition. Episodic fluid flow may be caused by the cyclic increase in pressure before a fracturing event and decrease in pressure immediately following the event. The growth of crystals along open fractures may block fluid flow by occluding the pore/fracture network. In this case fluid flow will only be held off until pressures increase enough to reactivate the fault or create a new one. Sibson (1994) discusses the cyclic time-scale of accumulation and release of stress in a hydrothermal system. He states that the build-up of shear stress during the inter-seismic period can last tens to many thousands of years. However, during a rupture, the drop in shear stress and subsequent fluid flow may last only a few seconds. This is followed by a period of "post-seismic adjustment" which may last for days to years.

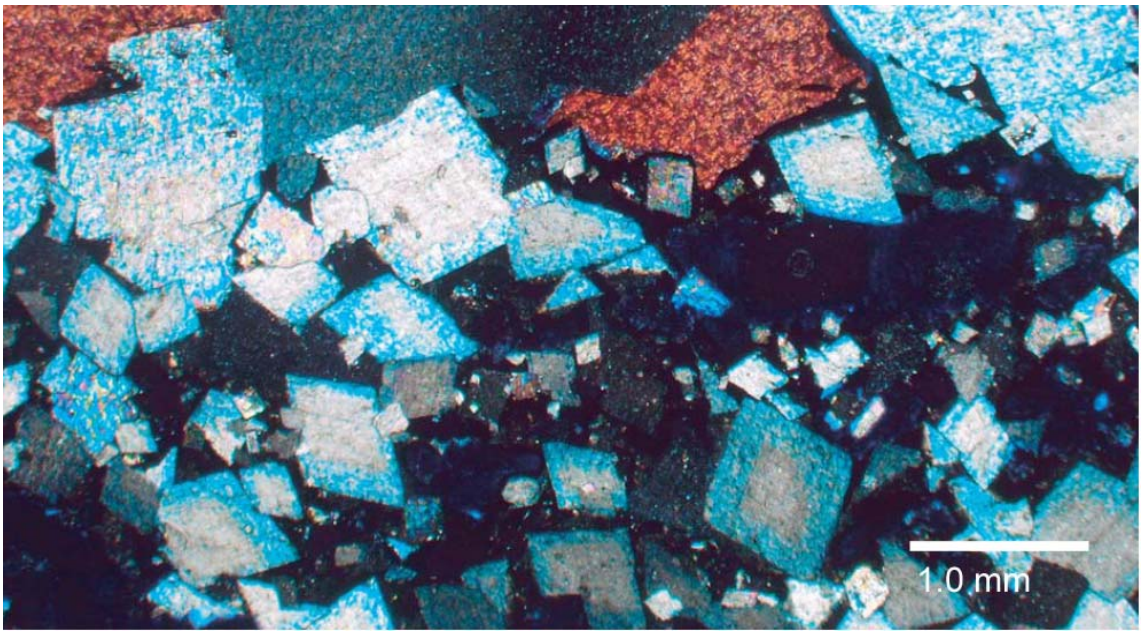

Figure 44 - Zoned saddle dolomite crystals

Taking this concept into consideration, the timing of formation for the Palatine Bridge Quarry outcrop is likely complicated and not restricted to a single event. As discussed in Chapter 2.3, most of the faulting in the Cambrian and Ordovician units of the Mohawk Valley is related to the Taconic Orogeny which occurred during the Late Ordovician (Bradley and Kidd, 1991). This collision may not have caused of the initial faulting beneath the quarry, but it certainly would have made a large contribution to the overall deformation. During this period of time the Tribes Hill formation was shallowly buried beneath the Black River, Trenton, and newly deposited Utica to an estimated depth of only 500-1500 feet Such a shallow depth could not account for the high T_H reported in the fluid inclusion analyses. Without an alternative source of heat, the fluids must have originated from a depth at which the geothermal gradient can account for these higher temperatures. Using the parameters laid out in Chapter 5.2, fluids with a temperature corresponding to the T_H in our samples (104-154°C) must have been buried

at least 5km (8mi) below the surface. This places the fluids below the Little Falls formation and well into the Precambrian basement. There is evidence for the reactivation of pre-existing basement faults during the onset of the Taconic Orogeny (Jacobi and Fountain, 2005). This is supported by the strontium data which suggests that these fluids traveled along fault lines rooted in basement structures deep enough to account for the thermal maturity of the dolomite fluid inclusions.

The core descriptions also support the interpretation that the Tribes Hill formation experienced faulting relatively early in its burial history. The soft sediment deformation and pressure solution observed in the cores verify that the unit was not fully lithified during the onset of tectonic activity. However, the extensive brecciation throughout the dolomite bodies is an indication that, at some point during its alteration, the rock was at least partially lithified. This contrast in evidence implies that dolomitization was episodic, occurring while the unit was soft, then again when hard. A separate collision is not necessary to explain this occurrence as the Taconic Orogeny took place over 40 million years which is more than enough time for the Tribes Hill to lithify. Paragenetic sequencing in thin sections show reactivation of bitumen filled fractures with an influx of late-stage calcite and quartz, however this event probably did occur during a later orogeny as there is no direct association between these minerals and the breccia. The system may have become reactivated during the Devonian Acadian Orogeny or the Carboniferous to Permian Alleghanian Orogeny.

5.3. Orientation and Structure of Faulting

Displacement in the study area is predominantly extensional, as seen in the normal faults of the fracture zone and central sag of the dolomite bodies. However, the origin of the stresses necessary to account for this deformation is likely much more complicated. The main problem with a purely extensional model is that 100% extension can not account for positive features such as the anticlines that flank the entire length of the dolomite bodies. A combination of transtensional stresses must be necessary to account for the all the characteristics observed throughout the study site.

Sandbox modeling of strike-slip pull-apart basins has revealed that lateral motion is not always recorded in slip along basin faults. In many cases, the faults surrounding a transtensional system may only show vertical offset, while lateral displacement occurs at greater depth (Dooley and McClay, 1997). Strike-slip motion along a releasing bend can create a relatively open space into which overlying units sink. As this deformation propagates upward, a negative flower structure consisting of normal fault displacement will form (Fig. 45). This system may also involve a component of reverse faulting along the edges of the basin as labeled in Figure 45. The flanking anticlines observed in the quarry may be a surface expression of this phenomenon. The cross-body scissor fault discussed in Chapter 4.3 also gives good evidence for a transtensional origin of the quarry fault and fracture system. Sandbox modeling of pull-aparts depict cross-basin scissor faults that change dip direction as they cross the "basin" (Fig. 45) (Dooley and McClay, 1994). The same research also describes the formation of relay ramp structures like the one seen in the quarry. Therefore, although the most common indications of strike-slip motion (horizontal slicken-sides or laterally offset markers) are absent from

the outcrop, the characteristics which are present fit into a transtensional regime very well.

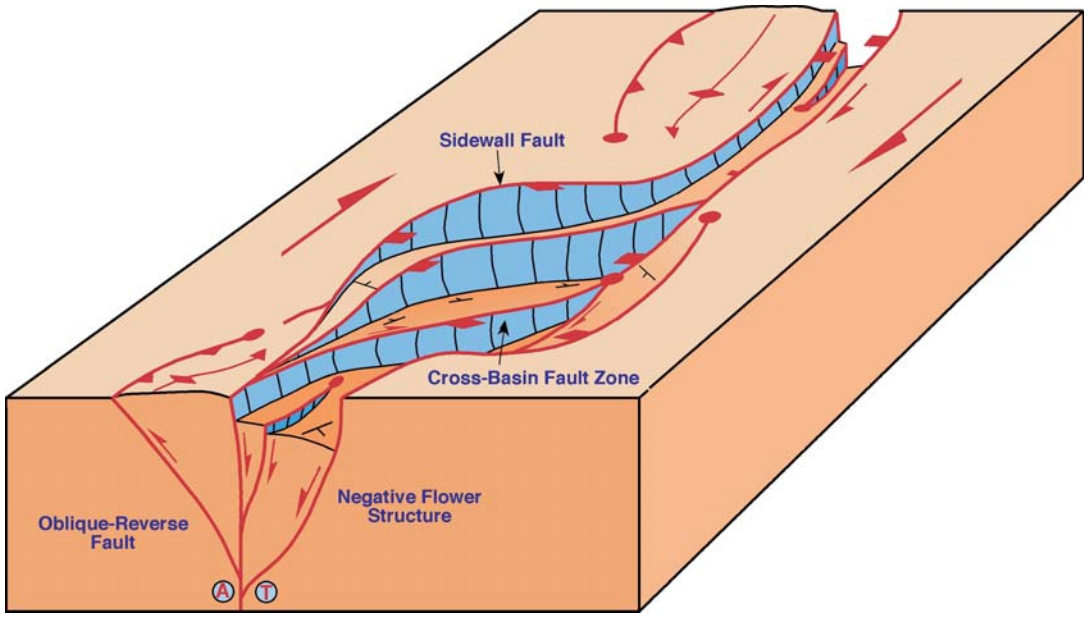

Figure 45 – Strike-slip pull-apart basin structure (Dooley and McClay, 1997)

Faults in the Mohawk Valley generally have three orientations: Northeast, North-South, and Northwest (Bradley and Kidd, 1991; Jacobi and Mitchell, 2002). With a strike of 305° (W-NW) the dolomite bodies of the quarry display a trend most closely related to the NW faults described by Jacobi, 2002. Although these faults were active during the Taconic Orogeny, they are believed to have an older history. Rifting associated with the opening of the Iapetus Ocean during the Eocambrain parallels the NE-striking fault system and is therefore thought to be related to the faulting. Consequently, transfer zones between the Iapetan rift segments may correspond to the NW-striking fault system and possibly the Palatine Bridge Quarry outcrop. The presence of low-cohesion faults that are well oriented for reactivation in the prevailing stress field will often become active before

new faults form (Sibson, 2000). Therefore, although these NW-striking transfer zones would have been characterized by pure strike-slip motion during their Cambrian formation, reactivation and upward growth into the overlying units during the Taconic Orogeny may exhibit motion concurrent with the stress field at that time, i.e. oblique strike-slip, or transtensional faulting.

Many of the structures in the quarry appear to match the work done by Sibson in his research of geodynamics and fluid involvement in faulting. He states that the interconnection of faults and fractures are directly related to the mechanical properties of alternating layers in a unit. Layers with a relatively high tensile strength such as sandstones or limestones typically undergo hydraulic extension fractures perpendicular to $\sigma_{3,}$ whereas layers with a lower tensile strength such as shales experience brittle shear failure. "Thus, in a typical sequence of alternating sandstones/limestones and shales, differences in tensile strength relative to the differential stress may result in the formation of a natural fault/fracture mesh" (Fig. 46b) (Sibson, 1994). The relict mesh structure is often preserved through cementation by mineralization of silica, carbonate, and bitumen (all present at the quarry). Many of the faults and fractures in the quarry display a similar pattern of shear failure across shaley beds while limestone layers contain extension fractures (Fig. 46a). Sibson states that the passage of large fluid volumes through these fault/fracture meshes leads to brecciation. As noted in Chapters 4.3 and 4.4, breccias are common in many sections of the outcrop. Figure 47 shows an idealized sketch of an extensional chimney, one type of fault/fracture mesh described by Sibson. Note that the cumulative offset along the shear zones creates a sag feature much like that seen in the quarry.

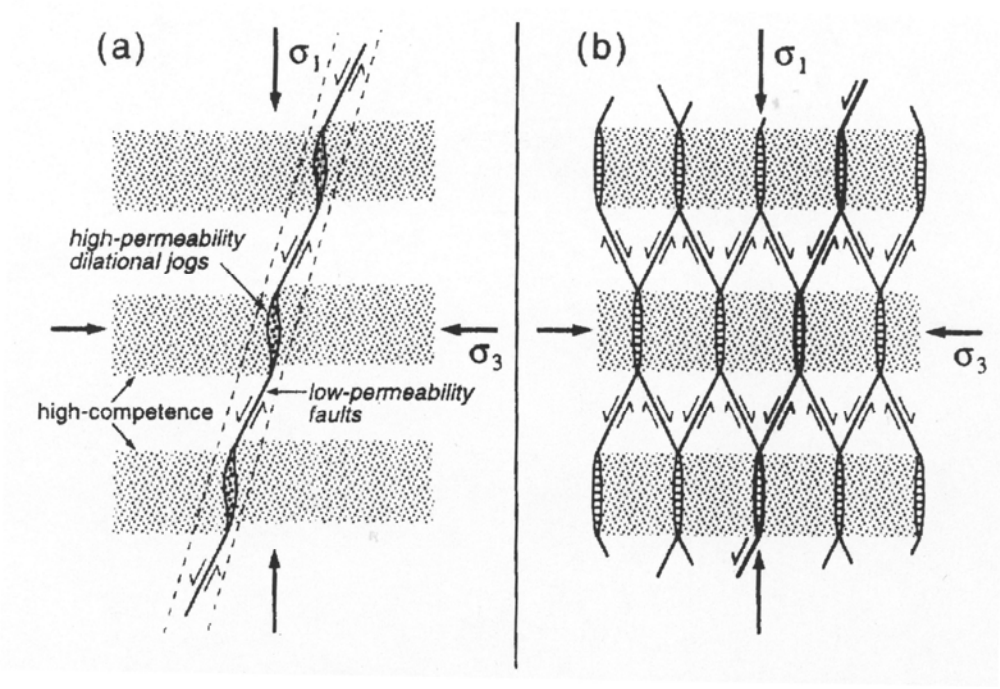

Figure 46 - a) Illustration showing the effect of alternating layers of competence on the formation of faults and fractures. b) Illustration of an idealistic fault/fracture mesh (Sibson, 1994)

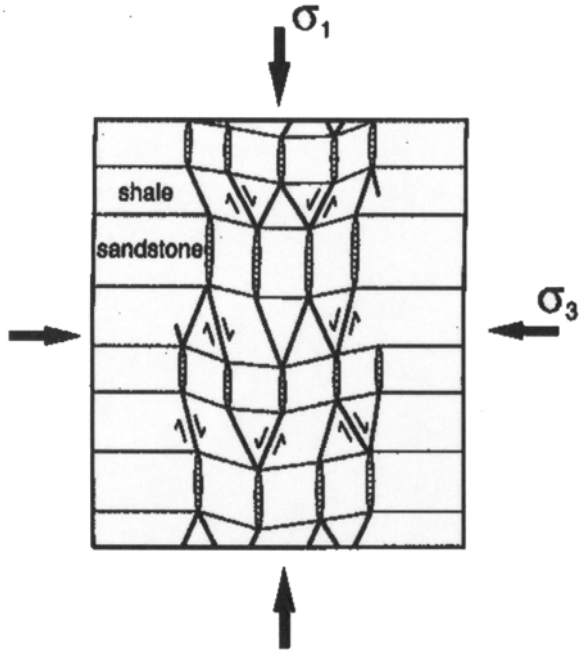

Figure 47 - Extensional chimney created by interconnected fault/fracture mesh (from Sibson 1994)

Several structures in the quarry also mirror the studies conducted by Childs (Childs, 1995 & 1996) in his work on fault overlap zones within developing segmented fault systems. Fault overlap zones, as described by Childs, are mostly temporary features. Unless growth of a fault ceases, overlap zones will eventually be breached forming transform zones or fault bends (Fig. 48). It is also important to note that overlap zones are spatially variable in that at one depth a pair of fault segments may exist as separate overlapping faults, but are joined at a stratigraphically higher or lower depth (Fig. 49). Similarly, the jog in middle of Body 2 may in fact be a breach between what were once two separate fault traces. The tail-like feature described in Chapter 4.3 may actually be a remnant tip of the eastern portion of Body 2 before it joined with the western portion. The geometry of this region is remarkably similar to that seen in the breached overlaps studied by Childs. It is also possible that the two halves of Body 2 may still have existed as separate bodies at a higher elevation which has since been eroded. On the same grounds, it is reasonable to presume Bodies 1 and 2 are connected at greater depth. Although the bodies themselves do not actually overlap, the calcite veins running from their tips do. We also know, from the analysis of Core 4, that the limestone bridge between these bodies is only four feet thick, beneath which dolomite occurs. This implies that Bodies 1 and 2 do actually meet at depth. Again, core analysis alone is not sufficient evidence for a complete structural interpretation, but future seismic work may help explain the way these bodies interact in the subsurface.

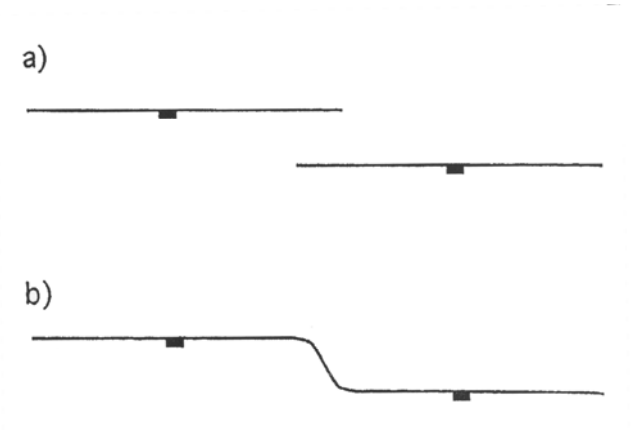

Figure 48 - a) fault overlap zone b) overlap breached creating a fault bend (Childs, 1995)

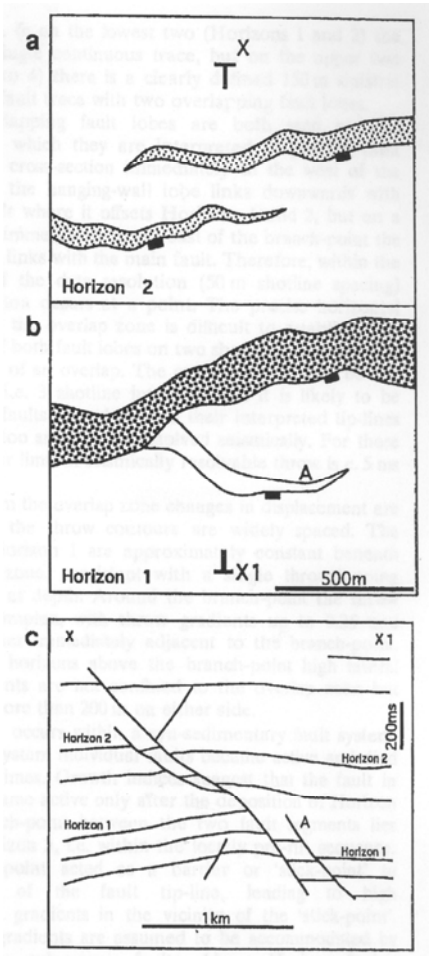

Figure 49 - a) illustration of fault overlap zone (horizon 2)
b) illustration of breached overlap with remnant tail (horizon 1)
c) profile view of fault interaction (Childs 1995)

5.4. Comparison to Producing Fields

As potential oil and gas reservoirs, occurrences of hydrothermal dolomite have gained increasing interest with each successful field discovered. Among the most productive of these fields are the Ladyfern Field of British Columbia, the Albion-Scipio fields in South-Central Michigan, and the Trenton - Black River fields of South-Central New York. Each of these fields shares a number of characteristics with the Palatine Bridge Quarry outcrop.

The Ladyfern Reservoir, discovered in 2000, was North America's largest onshore gas discovery in 20 years (Boreen and Davies, 2002). By the end of March 2002, the field consisted of 40 wells producing a total of 22 million m^3 of gas per day. Like the quarry outcrop, the Ladyfern reservoir is a fault controlled hydrothermal dolomite alteration. According to Boreen and Davies, "episodic burial reactivation of faults has resulted in extensive fracturing and created active conduits for hydrothermal fluids which have variably leached, dolomitized and cemented the rock. In areas of maximum extension near fault intersections, intense dissolution, brecciation and hydrothermal dolomitization has resulted in seismically-resolvable collapse synclines." In many ways, this description mirrors that of the Palatine Bridge dolomite structure. The same type of collapse synclines have been described and can be seen in the GPR data presented in Chapter 4.1. The leached rock texture and brecciation are also common characteristics between these two dolomite occurrences.

The Rochester Field is located in Southern Ontario, Canada, near Lake Erie just east of Detroit. It is one of the area's six major oil and gas pools, all of which produce from hydrothermally altered portions of the Trenton - Black River. As of 2005, the

Rochester Field had a cumulative oil production of 1.5 million bbl and a cumulative gas production of 1.45 bcf (Carter et al. 2005). The reservoir is associated with basement related flowered faults which compartmentalize the dolomite bodies (Ogiesoba, 2005). Figure 50 shows a horizontal slice of a 3-D seismic survey shot over the Rochester field. Note the geometric similarities between it and the quarry outcrop. Both are linear features that step in an en-echelon pattern. Figure 51 shows 2 cartoon cross sections of the field. They depict the same type of localized body and central sag as the trench walls and GPR data from the quarry.

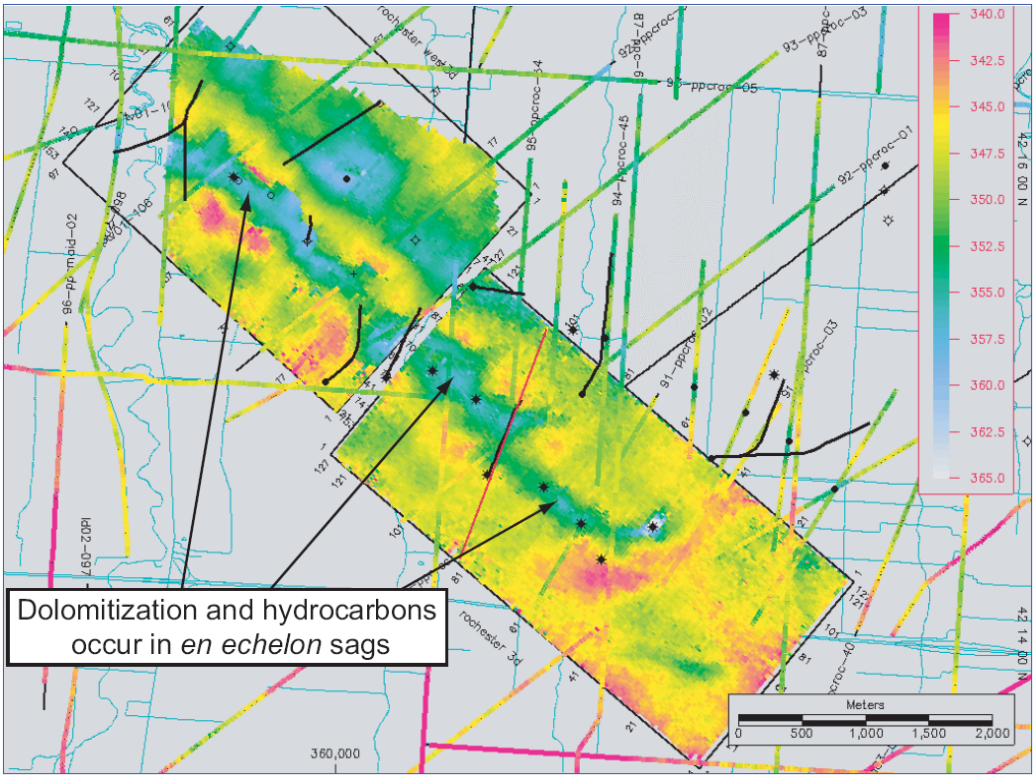

Figure 50 - Horizontal slice taken from 3-D seismic survey of the Rochester field, ONT

a)

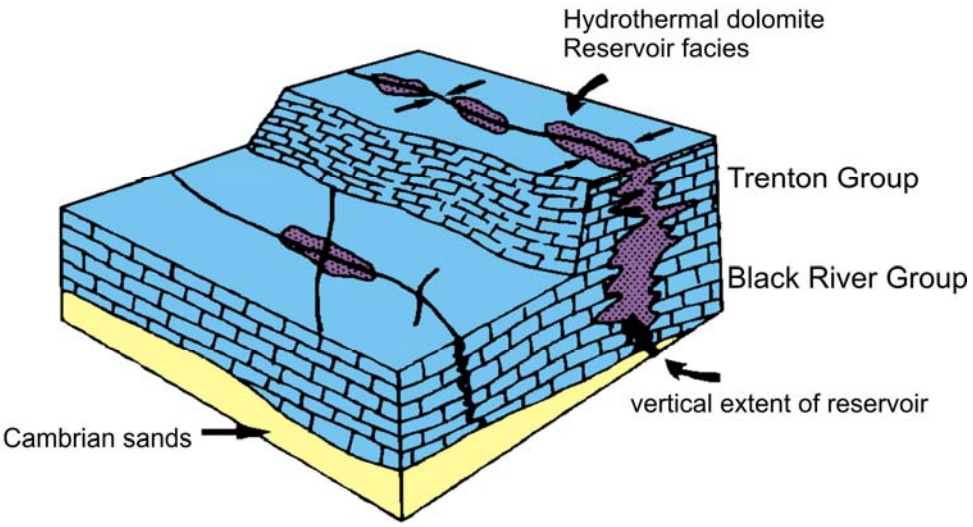

b)

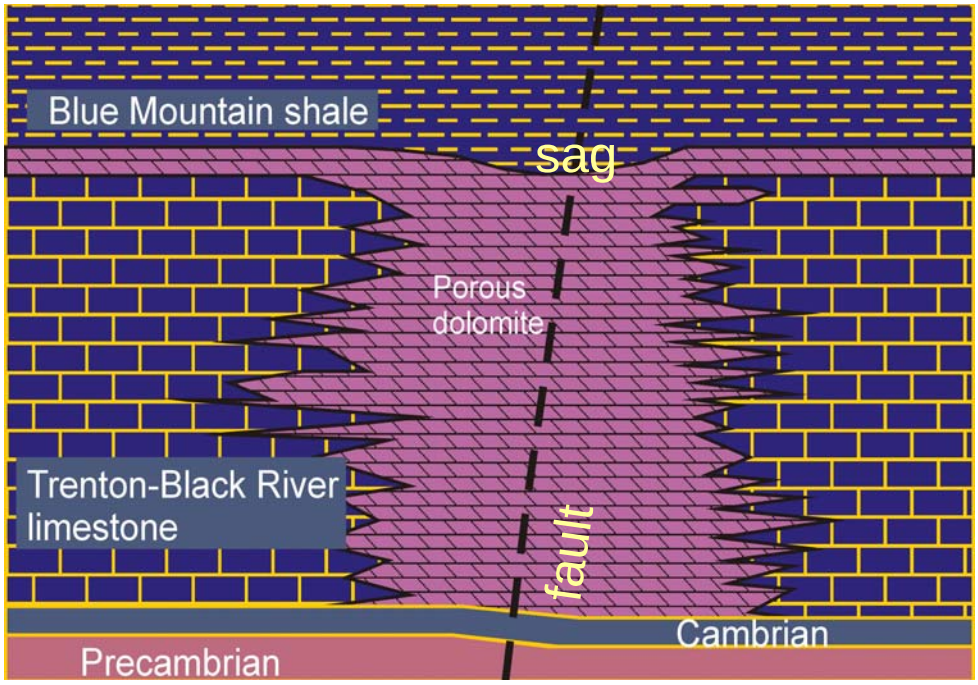

Figure 51 - cartoon cross-sections of dolomitization in the Rochester field (Carter, 1996)

The Albion-Scipio Fields of South-Central Michigan cover approximately 14,500 acres and also target hydrothermally dolomitized regions of the Trenton - Black River Formations. At the time of their discovery in 1957 these fields were estimated to contain over 290 million barrels of oil with a range of 10,000 to 25,000 barrels per surface acre (Hurley and Budros, 1990). They are considered "unusual" because, like Ladyfern, the hydrocarbon-bearing structures are synclinal sag-like features rather than the typical anticline trap. This sag is characteristic of most hydrothermal dolomite reservoirs and the Palatine Bridge outcrop. Perhaps the most interesting element of the Albion-Scipio Fields is that not only do they resemble the quarry bodies in cross-section, but in plain view as well. The Albion-Scipio Fields occur as long, linear en-echelon segments (Fig. 52). Note the Pulaski Break between these fields bears a striking resemblance to the bridge between bodies 1 and 2 at the quarry. And although their orientation differs, the bend in the Scipio field looks much like the jog in Body 2 at the quarry. In fact, when reflected vertically and placed next to the Rochester and Albion-Scipio outlines, all three structures display the same geometry (Fig. 53). Other similarities between the Michigan fields and New York study area include vuggy porosity, brecciation, and occurrences of saddle dolomite, calcite, and pyrite.

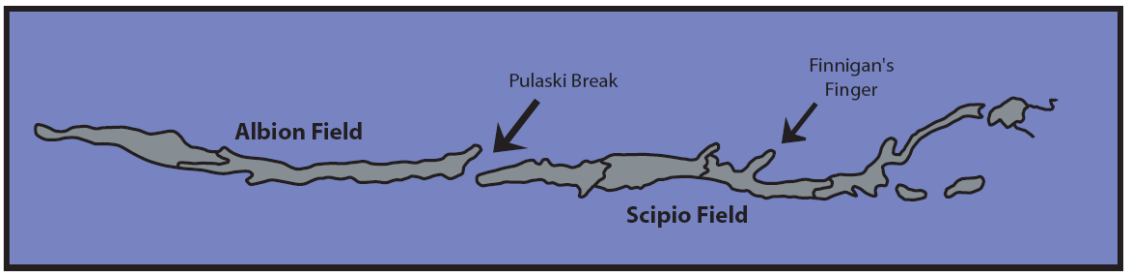

Figure 52 - Illustration of Albion - Scipio fields in map view (digitized from Hurley and Budros, 1990)

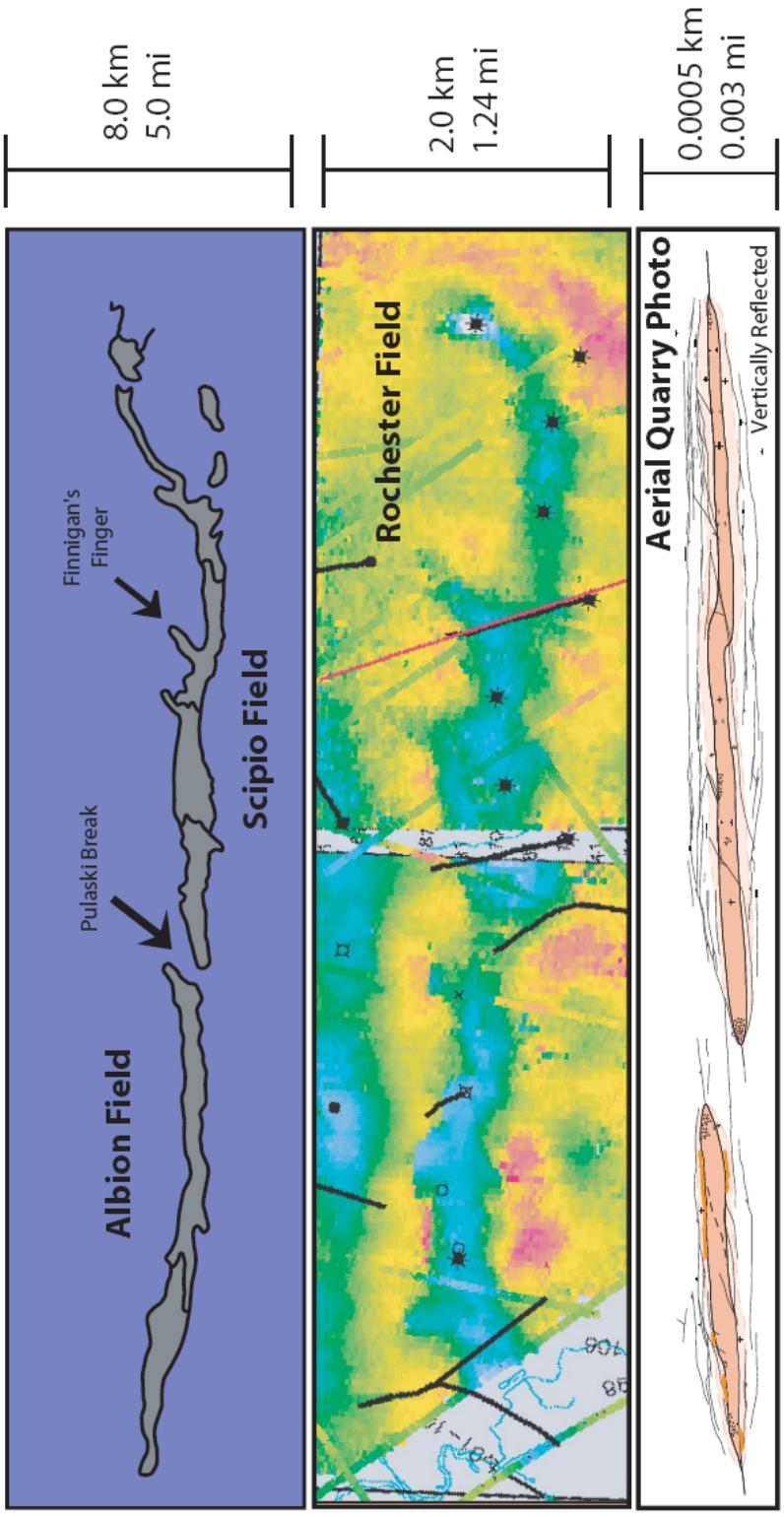

Figure 53 - Comparison of Albion - Scipio field and Rochester field to vertically reflected quarry fracture map

Like the Albion-Scipio Fields of Michigan and the Rochester Field of Ontario, a large portion of the hydrocarbon production in New York targets the Trenton - Black River play. Fields such as Quackenbush Hill and Wilson Hollow produce natural gas from hydrothermally dolomitized sections of these formations. These fields contain wells that are known to produce up to 6,474,551 MMCFG. In map view, the fields appear as elongate fault-bounded structural lows (Fig. 54) (Smith, 2006). Geochemical analysis of cores taken from these fields yield $\delta^{18}O$ values between -9 and -12.5‰ (Smith, 2006). Values from the quarry lie in the same range (see Chapter 4.6). The cores also show elevated strontium content much like the quarry samples and vuggy porosity with saddle dolomite like the quarry cores and outcrop.

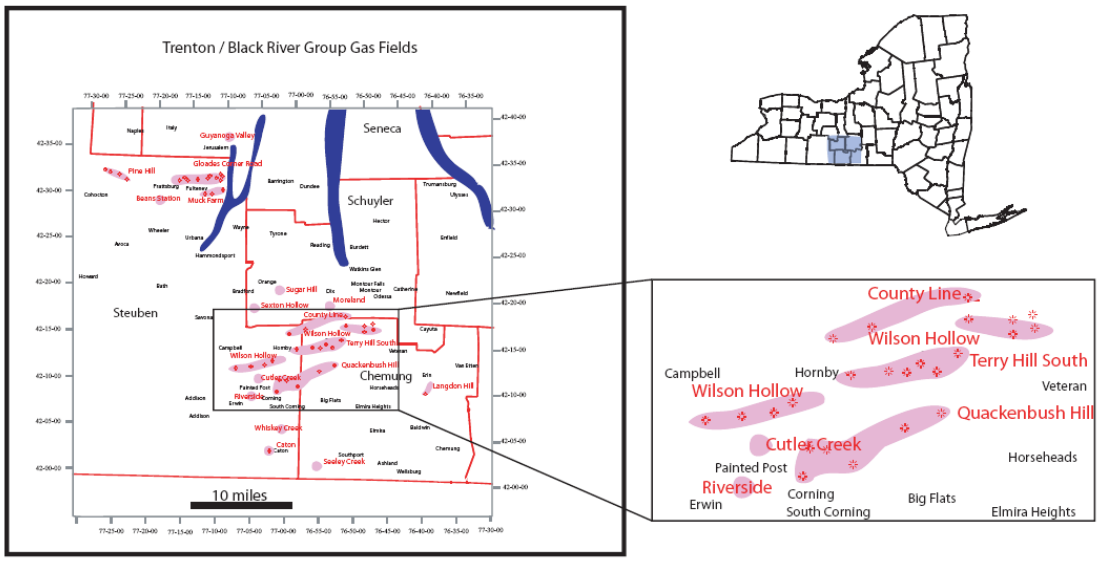

Fig. 54 - Trenton / Black River hydrothermal dolomite fields of south - central New York as of 2003

Chapter 6 – Conclusions

As stated in Chapter 1.1, there were three main objectives of this study. The first of these goals was to confirm the hydrothermal origin of the Palatine Bridge outcrop. Unfortunately, homogenization temperatures of fluid inclusions in the dolomite are definitively higher than the maximum ambient burial temperature of the Tribes Hill in NY. Therefore, the outcrop cannot be said to be unequivocally hydrothermal. However, all other characteristics of the quarry point to fault related fluid flow and precipitation of crystals at temperatures higher than the shallowly buried Tribes Hill during the Taconic Orogeny. Both GPR and core analysis show that the outcrop is directly associated with faults and fractures. Even the size and geometry of the bodies eliminate many other possible methods of dolomitization. Elevated strontium content indicates that the parent fluid interacted with the Precambrian Basement before precipitation of dolomite. This could only mean that the fluids came from a greater depth and would consequently have been hotter than the rock they intruded. By a simple process of elimination, hydrothermal alteration of the Tribes Hill is the only way these dolomite bodies could have formed.

The second objective of this project was to constrain the timing of dolomitization. This matter is complicated by the issue of reactivated faults and episodic fluid flow. As discussed in Chapter 5.3, the faults were probably pre-existing transfer zones from Iapetan rifting. Reactivation during the Taconic Orogeny (Mid-Late Ordovician) while the Tribes Hill was still shallowly buried would explain the soft sediment deformation seen in the cores. An upper limit on the timing of faulting is constrained by the

termination of these faults in the Trenton and Utica formations. However, the coexistence of soft sediment deformation and brecciation implies that the faulting was episodic and occurred while the sediment was soft then again later after it had hardened. Multiple tectonic events including the Taconic, Acadian, and Alleghanian Orogenies must have been involved.

The third and final goal of this study was to confirm the value of the Palatine Bridge outcrop as an analog for Trenton - Black River fields. This objective was met through the comparison and discussion in Chapter 5.5. The geometric similarities are the most obvious characteristics shared by the quarry and producing fields. These structures occur as long, linear en-echelon bodies characterized by an anticline-flanked sags overlying basement rooted faults. Vuggy porosities, brecciation, and mineral assemblages also help link the study area to its larger counterparts. Finally, the geochemical signature of the quarry dolomite is virtually identical to that of the producing fields of south central New York. Therefore, although their scales differ greatly, the Palatine Bridge outcrop may be studied as an analog for larger hydrothermal dolomite bodies in exploration for future oil and gas production prospects.

Bibliography

Akcay, M., Ozkan, H.M., Spiro, B., Wilson, R., Hoskin, P.W.O., 2003, Geochemistry of High-T hydrothermal dolostone from the Emirli (Odemis, western Turkey) Sb-Au deposit: Mineralogical Magazine, v.64, p. 672 - 688.

Allan, J.R., Wiggins, W.D., 1993, Dolomite reservoirs: geochemical techniques for evaluating origin and distribution: AAPG Continuing Education Course Note Series, 36, p. 169.

Auajjar, J., Boulegue, J., 2002, Dolomites in the Tazekka Pb-An district, eastern Morocco: polyphase origin from hydrothermal fluids: Terra Nova, v.14, n.3, p. 175 - 182.

Berg, W.F., 1938, Crystal growth from solutions: Proceedings Royal Society London, Series A, v.164, p. 79 - 95.

Boreen, T., Davies, G., 2002, Hydrothermal Dolomite and Leached Limestones in TCF Gas Play: the Laydfern Slave Point Reservoir, NEBC: abstract from 2004 Dolomite Conference, The Spectrum: Mechanisms, Models, Reservoir Development.

Bradley, D., Kidd, W.F.S., 1991, Flexural extension of the upper continental crust in Collisional foredeeps: Geological Society of America Bulletin 103, no.11, p. 1416-1438.

Braithwaite, C.J.R., Rizzi, G., 1997, The geometry and petrogenesis of hydrothermal dolomites at Navan, Ireland: Sedimentology 44, no.3, p. 421 - 440.

Burke, W.H., 1982, Variation of seawater Sr^{87}-Sr^{86} throughout Phanerozoic time: US Geological Survey Bulletin 1529E, p. 16

Carter, T., McFarland, S., Trevail, R.A., Gorman, J., Philip, W., 2005, Trenton-Black River Hydrothermal Dolomite Reservoirs in Ontario: Geology, Reserves and Potential Resources: 2005 AAPG Annual Convention.

Childs, C., Watterson, J., Walsh, J.J., 1995, Fault overlap zones within developing normal fault systems: Journal of the Geological Society, London, v.152, p. 535 - 549.

Childs, C., Nicol, A., Walsh, J.J., Watterson, J., 1996, Growth of vertically segmented normal faults: Journal of Structural Geology, v.18, n.12, p. 1389 - 1397.

Davies, G., Smith, L., 2006, Hydrothermal Structurally controlled hydrothermal dolomite reservoir facies: An overview: 2006 AAPG Bulletin 90, no.11, p. 1641 – 1690.

Fisher, D.W., 1954, Lower Ordovician (Canadian) stratigraphy of the Mohawk Valley, New York: Geological Society of America Bulletin 65, p. 71 - 96.

Goldstein, R.H., Reynolds, J. T., 1994, Systematic of fluid inclusions in diagenetic minerals: SEPM short course 31. 199p.

Hill, D.P., 1977, A model for earthquake swarms: Journal of Geophysical Research 82, p. 1347 - 1357.

Hulver, M. L., 1997, Post-orogenic evolution of the Appalachian basin mountain system and its foreland: Ph.D. thesis, University of Chicago, Chicago, Illinois, p. 917.

Hurley, N.F., Budros, R., 1990, Albion-Scipio and Stoney Point Fields - USA, Michigan Basin: Treatise of Petroleum Geology Atlas of Oil and Gas Fields, The American Association of Petroleum Geologists, Tulsa, OK.

Jacobi, R., 1981, Peripheral bulge - a causal mechanism for the Lower/Middle Ordovician unconformity along the western margin of the northern Appalachains: Earth and Planetary Science Letters 56, p.245 - 251.

Jacobi, R., 2002, Basement faults and seismicity in the Appalachian Basin of New York State: Tectonophysics 353, n.1-4, p.75 - 113.

Jacobi, R., Fountain, J., 2005, The character and reactivation history of the southern extension of the seismically active Clarendon-Linden Fault system, western New York State: Tectonophysics 353, no.1-4, p.215 - 262.

Joy, M.P., 2000, Evidence of a tectonically driven sequence succession in the Middle Ordovician Taconic foredeep: Geology 28, no.8, p. 727 - 730.

Landing, E., 1996, Conodonts, stratigraphy, and relative sea-level changes of the Tribes Hill Formation (Lower Ordovician, east-central New York): Journal of Paleontology 70, no.4, p. 656 - 680.

Loucks, R., McMechan, G., 1998, Ground penetrating radar imaging of a collapsed paleocave system in Ellenburger dolomite, central Texas: Journal of Applied Geophysics, v. 39, p.1 - 10.

Ogiesoba, O.C., 2005, Fault-Controlled Porosity Within a Trenton-Black River Hydrothermal Dolomite Reservoir: abstract from AAPG Annual Convention Technical Program.

Peacock, D.C.P., Knipe, R. J., Sanderson, D.J., 2000, Journal of Structural Geology 22, no.3, p. 291-305

Sibson, R.H., 1994, Crustal stress, faulting and fluid flow: Geological Society Special Publication, no.78, p. 69 - 84.

Sibson, R.H., 2000, Fluid involvement in normal faulting: Journal of Geodynamics 29, p. 469 - 499.

Smith, L., 2006, Origin and Reservoir Characteristics of Upper Ordovician Trenton-Black River Hydrothermal Dolomite Reservoirs in New York, USA: AAPG Bulletin 90, no.11, p. 1691 - 1718.

Warren, J., 2000, Dolomite: Occurrence, evolution and economically important associations: Earth Science Reviews 52, no.1-3, p. 1 - 81

Weary, D.J., Ryder, R.T., Nyahay, R.E., 2001, Thermal Maturity Patterns in New York State Using CAI and $\%R_o$: Northeastern Geology and Environmental Sciences, vol.23, no.4, p. 356 - 376.

White, D.E., 1957, Thermal waters of volcanic origin: Geological Society of America Bulletin, V.68, p. 1637 - 1658.

Zenger, D.H., Dunham, J.B., Ethington, R.L., 1980, Concept and models of dolomitization: Society of Economic Paleontologists and Mineralogists Special Publication 28, p. 1 - 9.

Zenger, D.H., 1981, Stratigraphy and Petrology of the Little Falls Dolostone (Upper Cambrian), East-Central New York, New York State Museum Map and Chart Series 34, 138p.

Appendices

Appendix 1. Richard Bray's Core Descriptions

HOLE 1

Little Falls Formation

38.8-24.1 ft.

Little Falls-Tribes Hill Transitional Beds

24.1-22.9 ft.
Brownish gray and medium gray, silty dolostone. Bedded mudstone. Rare to sparse microstylolites. Rare horizontal burrows. Large bitumen- and pyritized bitumen-filled fracture. Small, dolomite-filled fracture. Sparse pyrite outside fracture. Fractures exhibit little displacement. Patchy, intercrystalline porosity is restricted to individual beds. Rare porosity in horizontal burrow partially cemented with dolospar. Upper surface of the unit is undulatory.

Tribes Hill Formation

Unit 1: 22.9-22.5 ft.
Medium light gray, slightly argillacous, silty dolostone. Crinkly laminated mudstone. Rare moldic or vuggy porosity.

Unit 2: 22.5-22.4 ft.
Medium dark gray dolostone and dusky yellowish brown, pyritic dolostone. Intraclastic packstone (?). Abundant bitumen. Large intraclasts often preserved as pyrite. Rare glauconite in the pyrite deficient dolostone.

Unit 3: 22.4-21.2 ft.
Brownish gray, silty argillacous dolostone. I*n situ* breccia (pseudobreccia) composed of numerous mudstone clasts. Pressure solution appears to have removed matrix. Common microstylolites. Rare shelter voids. Common pyrite. Rare vuggy or moldic porosity.

Unit 4: 21.2-19.6 ft.
Brownish gray and olive gray, silty dolostone. Bedded to lenticular mudstone. Sharp transition to olive gray dolostone at the 20.1 ft., apparently is a flat pebble conglomerate. Sparse pyrite. Fracture from 20.1-20.4 ft. propped open with pyrite. Rare intercrystalline porosity.

Unit 5: 19.6-17.8 ft.
Brownish gray to olive gray, slightly argillaceous to argillaceous, silty dolostone. The top of this interval is a well-defined, undulatory surface, apparently a dolomitized intraclastic grainstone. Original textures, which have largely been obliterated by intense dolomitization, are not immediately apparent. Bedding appears to be largely horizontal. Scattered clasts and horizontal burrows locally are identifiable. Local concentrations of microstylolites provide evidence of "ribbon rock" and nodular textures. Rare to sparse intercrystalline and vuggy porosity.

Unit 6: 17.8-11.7ft.
Brownish gray silty, argillaceous dolostone. Bedding horizontal, although original textures obscure due to intense dolomitization. Rare microstylolite swarms. Well-developed intercrystalline and vuggy porosity.

Unit 7: 11.7-0.0 ft.
Brownish gray, olive gray and olive black silty, argillaceous dolostone. Fracture zone between 7.2-10.0 ft. Brecciated, deformed strata. Bedding is vertical to slightly inclined. Fabrics appear streaked, probably ductiley deformed. Numerous breccia clasts lack well-defined margins. Silt and clays are abundant. Porous fabrics, although very rare, has well-developed intercrystalline and vuggy porosity.

HOLE 2

Little Falls Formation

54.0-24.6 ft.

Little Falls-Tribes Hill Transitional Beds

24.6-23.6 ft.
Brownish gray slightly argillaceous and silty dolostone. Bedded mudstone. Some beds, which are lenticular, contorted and not continuous, were probably affected by soft sediment deformation. Rare high angle, bitumen-filled fracture near base continues into the Little Falls Formation. Sparse to rare burrows, especially immediately above base. Rare microstylolites. Rare pyrite. Upper contact is an undulatory surface.

Tribes Hill Formation

Unit 1: 23.6-23.2 ft.
Medium light gray and medium gray slightly argillaceous, silty dolostone. Crinkly laminated mudstone. Conspicuous dark gray interbed near middle. Numerous gravel sized intraclasts. Trace echinoderms. Some laminae are fragmented *in situ* at base. Rare to sparse vuggy porosity in the upper third of the unit.

Unit 2: 23.2-23.0 ft.
Brownish gray dolostone. Intraclastic packstone with thin mudstone drape. Intraclasts not distinct. Diffuse glauconite above mudstone drape. Sparse intergranular porosity associated with the intraclast-rich portions.

Unit 3: 23.0-21.6 ft.
Light brownish gray and brownish gray silty dolostone: I*n situ* breccia (pseudobreccia), which is somewhat obscured by dolomitization. Interbedded, light, early cemented mudstone bed and dark, organic-stained, silty muds. Bioturbation also disrupts bedding. Rare cemented shelter voids. Sparse fracture porosity associated with early fractures of mudstone chips. Sparse vuggy porosity in the beds which were not cemented syndepositionally. Rare moldic and vuggy pores in dolomitized mud chips.

Unit 4: 21.6-20.2 ft.
Medium dark gray and medium gray dolostone silty dolostone. Mudstone interbedded with thin cross-laminated grainstones. Laminated beds and lenticular beds near top. Rare calcite-cemented fractures. Rare small intraclasts. Rare wispy microstylolites. Rare clays. Rare pyrite. Silt more common in cross laminated beds. Intercrystalline porosity restricted cross-laminated beds. Flat pebble conglomerate with cemented shelter voids at top of interval.

Unit 5a: 20.2-17.8 ft.
Brownish gray, olive gray and medium dark gray dolostone and argillaceous, silty dolostone. "Ribbon rock" which is somewhat obscured by dolomitization. Common microstylolites. Mudstone? Rare pyrite. Well-developed, intercrystalline porosity (approximately 10-15%).

Unit 5b: 17.8- 16.6 ft.
Brownish gray, argillaceous, silty dolostone and white saddle dolospar cement. A conspicuous hydrothermally fractured/brecciated zone cemented with saddle dolomite. Later coarse, calcite spar is rare. Common vuggy, intergranular (between breccia clasts) and intercrystalline porosity. Pores, several centimeters in diameter, are associated with the intergranular voids.

Unit 5c: 16.6-16.0 ft.
Brownish gray, olive gray and medium dark gray dolostone and argillaceous, silty dolostone. "Ribbon rock" , which is somewhat obscured by dolomitization. Similar in most respects to Unit 5a, except less intercrystalline and vuggy porosity.

Unit 6: 16.0-12.6 ft.
Brownish gray and medium dark gray sandy (very fine), slightly calcitic dolostone grading quickly upward to silty, dolomitic limestone at top. Perhaps a less distinct "ribbon rock". Calcitic portion appear to be wackestone to muddy packstone. Trilobites, echinoderms and intraclasts, peloids and echinoderms are most common carbonate grains. Brachiopods and bivalve mollusks are rare. Rare echinoderms. Rare saddle dolomite (at base). Replacement dolomitization (medium crystalline-replacement) is patchy and not obviously fabric selective. Sparse to common pyrite. Wispy microstylolites appear to concentrate silt. Some beds or intraclasts have fine, calcite-filled syndepositional fractures. Rare to sparse calcite-cemented horizontal burrows, especially conspicuous near top of interval.

Unit 7: 12.6-0.0
Olive gray, light brownish gray, medium light gray and medium dark gray dolomitic limestone. "Ribbon rock". Wackestone and the rare packstone and grainstone. Thin, non-skeletal grainstones may have eroded tops. Limestone interbeds generally less than 5 centimeters. Limestone of the nodular intervals generally mudstone. Intervening matrix-rich beds often no more than dense microstylolite swarms, which locally may be argillaceous. Several packstone beds composed of large intraclasts. Grainy interbeds dominated by non-skeletals (intraclasts, rare peloids) and rarer skeletals (trilobites). Algal fragments (Ortonella?) are locally present. Intraclasts may have blackened rim. Some intraclasts have thin, syndepositional calcite-filled fractures. Rare stylolites. Replacement dolomite is locally abundant. Rare horizontal burrows often filled with fine dolomite replacement. Rare to sparse pyrite. Fractures at 3.0-3.1 ft. and 5.3-6.3 ft. filled with saddle dolomite. Later calcite spar fills fracture at 5.3-6.3 ft.. Fracture and breccia at 7.1-7.5 ft. cemented with saddle dolomite and later calcite spar. All fractures and

breccia show little displacement. Sparse, large intercrystalline pores (up to 2 millimeters) associated with saddle dolospar.

HOLE 3

Little Falls Formation

55.0-24.6 ft.

Little Falls-Tribes Hill Transitional Beds

24.6 -23.7 ft.
Light brownish gray and brownish gray silty dolostone. Bedded and laminated mudstone. Rare horizontal and vertical burrows. Bitumen- and dolospar-filled fracture (24.3-24.6 ft.). Sparse, low amplitude stylolites. Rare pyrite. Rare fracture porosity and trace moldic porosity.

Tribes Hill Formation

Unit 1: 23.7-23.3 ft.
Light brownish gray argillaceous, silty dolostone. Crinkly, laminated mudstone. Several thin argillaceous rich beds with dolomitized intraclasts and skeletals. Rare pyrite. Rare burrows.

Unit 2: 23.3-23.0 ft.
Light brownish gray dolostone. Intraclastic packstone (?). Intraclasts angular. Rare pyrite. Rare glauconite. Perhaps a thin hard ground and algal mat stabilizing top. Sparse to common moldic and vuggy porosity.

Unit 3: 23.0-21.7 ft.
Light brownish gray and brownish gray and silty, argillaceous dolostone. I*n situ* breccia (pseudobreccia) composed of numerous mudstone clasts, some undisturbed beds and imbricated flat pebble conglomerate at very top. Saddle dolospar partially occludes larger pores. Rare pyrite. Well-developed vuggy, moldic and intercrystalline porosity especially near base of unit. Largest pore approximately 3 millimeters.

Unit 4: 21.7-20.5 ft.
Medium gray and brownish gray, silty dolostone. Bedded to lenticular mudstone with conspicuous laminated portions. Upper surface irregular. Flat pebble conglomerate near top of unit. Irregular surface at 21.3 ft.. Rare bitumen- and dolospar-filled vugs. Rare microstylolitic seams and stylolites. Large, open fracture, which is partly occluded by pyrite and dolospar, extends from top of unit to 21.2 ft.. Rare vuggy porosity associated with the flat pebble conglomerate.

Unit 5: 20.5-17.9 ft.
Olive gray, silty, slightly argillaceous dolostone. “Ribbon rock” and nodular fabric of interbedded dolostone and silty, argillaceous dolomitic, microstylolitic seams. Depositional texture obliterated by dolomitization. Numerous microstylolites. Scattered

intraclasts. Rare horizontal burrows near base of unit. Rare pyrite. Excellent intercrystalline and vuggy porosity. Largest pore approximately 1 millimeter.

Unit 6: 17.9-17.2 ft.
Olive gray, slightly silty dolostone. Primary depositional texture not immediately apparent. Probably an intraclastic packstone. Many voids cemented with saddle dolospar. Very good intercrystalline and vuggy porosity. Largest pore approximately 2 millimeters.

Unit 7: 17.2-7.1 ft.
Light brownish gray, brownish gray and medium dark gray silty, argillaceous dolostone. Primary depositional texture not apparent although probably a "ribbon rock" with an especially dense concentration of microstylolites at top of unit. Sparse pyrite. Excellent intercrystalline and vuggy porosity. Largest pore 1 millimeter.

Unit 8: 7.1-0.0 ft.
Brownish gray, silty, argillaceous dolostone. Dolomitization and diagenesis has obscured primary depositional fabric. Some micro zebra fabrics. Numerous breccia clasts throughout the interval. Rare, small (<1 millimeter) calcite-filled fractures. Rare intercrystalline porosity.

HOLE 4

Little Falls Formation

55.0-24.9 ft.

Little Falls-Tribes Hill Transitional Beds

24.9-24.3 ft.
Light brownish gray, silty dolostone. Rare organic-filled fractures. Thinly bedded mudstone. Some beds are contorted . Rare burrows. Rare microstylolites. Rare pyrite near top of unit. Undulatory upper surface.

Tribes Hill Formation

Unit 1: 24.3-24.0 ft.
Light brownish gray to brownish gray, silty, argillaceous, dolostone. Crinkly laminated mudstone and thinly bedded mudstone. Rare burrows. Numerous, thin, silty, argillacous laminae. Laminae fragmented *in situ* at base. Sparse microstylolites that concentrate silt and clay. Rare pyrite. Irregular, undulatory upper surface.

Unit 2: 24.0-23.9 ft.
Light brownish gray and medium dark gray dolostone. Probable intraclast packstone to grainstone. Rounded very coarse sand and gravel sized intraclasts. Pyrite abundant at base of unit. Rare glauconite. Sparse vuggy and moldic porosity.

Unit 3: 23.9-22.7 ft.
Brownish gray and olive gray silty, argillaceous, dolostone. I*n situ* breccia (pseudobreccia) composed of angular clasts. Rare pyrite. Numerous stylolitized grain contacts, which are near top of unit, indicate vertical as well as horizontal pressure solution. Rare intercrystalline and fracture porosity.

Unit 4: 22.7-21.0 ft.
Brownish gray, light brownish gray and olive gray silty dolostone. Bedded mudstone. Conspicuous, porous, flat pebble conglomerate at the top. Pressure solution has created numerous vertical stylolites and obscured the character of the bedding. Common pyrite disseminated in the matrix and concentrated along stylolites, probably as pyritized bitumen in the latter. Saddle dolomite cement partially fills large voids in the flat pebble conglomerate at the top. Porosity associated with stylolites and best developed in the flat pebble conglomerate at the top of the unit. Largest pore 1 millimeter.

Unit 5: 21.0-14.4 ft.
Olive gray and brownish gray slightly argillacous, silty dolostone. Deformation and dolomitization have largely obliterated the depositional fabric, although lack of microstylolite swarms indicate the unit largely consists of bedded carbonates. Beds are brecciated and often inclined. Microstylolites traces are rare. Sparse large voids partially

cemented with saddle dolospar and later, rare calcite spar. Intercrystalline, vuggy and, perhaps, moldic porosity generally well developed. Largest pores approximately 1 millimeter.

Unit 6: 14.4-10.2 ft.
Olive gray, silty, argillaceous dolostone. Deformation, brecciation and dolomitization have largely obliterated the depositional fabric, although abundance of microstylolite swarms indicate the unit largely consists of "ribbon rock" and nodular carbonates. Beds are brecciated or inclined. Microstylolites traces are common. Some microstylolites, beds and breccia clasts appear stretched or smeared, probably ductiley deformed. Saddle dolospar and later calcite spar fill or partially fill larger pores. Fracture trace between 11.1-12.0 ft.. Porosity commonly developed as vuggy and intercrystalline voids. Largest pores up to 1 millimeter.

Unit 7: 10.2-8.1 ft.
Brownish gray and olive gray, silty, argillaceous dolostone. Bedded carbonate, presumably deposited as limestone. Little or no disruption of beds. Rare microstylolites. Prominent surfaces at 8.3 and 8.5 ft.. Intraclasts at the very top. Rare to sparse vugs and intercrystalline pores.

Unit 8: 8.0-3.1 ft.
Brownish gray and olive gray, very silty, very argillaceous dolostone. Dolomitization obscures the depositional texture of this unit. Apparently little disruption of beds by faulting. The basal portion of the unit (6.9-8.1 ft.) appears disturbed, but disruption most probably related to deposition. Often the fabric displays a linearity, perhaps a microzebra fabric reflecting an alignment of the dolomite crystals. There is some inclined zebra fabric immediately below the sharp, irregular contact with the overlying limestone. Vuggy and intercrystalline porosity is rare to sparse and not uniformly developed throughout the unit.

Unit 10: 3.1-0.0 ft.
Olive gray, silty, argillaceous, slightly dolomitic limestone. "Ribbon rock" and nodular fabric of interbedded limestone and silty, argillaceous microstylolitic seams. Limestone beds up to 5 centimeters. Limestone interbeds generally are mudstone and wackestones with several thick intraclast packstone beds. Many intraclasts are mudstone and have a blackened rims. Intraclasts, peloids and echinoderms are the most common carbonate grains. Some stylolitized contacts between beds and intraclasts near the base of the unit. More dolomitic near basal contact with underlying dolomitized beds.

HOLE 5

Little Falls Formation

73.0-24.2 ft.

Little Falls-Tribes Hill Transitional Beds

24.2-23.2 ft.
Light brownish gray and brownish gray silty dolostone. Bedded and laminated mudstone. Bitumen-defined laminae at the very top. Several irregular surfaces, clotted fabrics and wavy bedding. Horizontal burrows immediately below two irregular surfaces.

Little Falls Formation

Unit 1: 23.2-22.8 ft.
Light brownish gray argillaceous, silty dolostone. Crinkly laminated mudstone.

Unit 2: 22.8-22.7 ft.
Light brownish gray dolostone. Intraclastic packstone (?). Sparse pyrite. Rare glauconite at the upper surface. Sparse vuggy porosity

Unit 3: 22.7-21.0 ft.
Light brownish gray, brownish gray and medium gray silty, argillacous dolostone. I*n situ* breccia (pseudobreccia) composed of numerous mudstone clasts and some undisturbed beds. Common pyrite, especially in more porous portion. Saddle dolospar and calcite spar partially occlude larger pores. Common vuggy, moldic and intercrystalline porosity. Largest pore approximately 2 millimeters.

Unit 4: 21.0-19.6 ft.
Medium gray to brownish gray and olive gray, silty dolostone. Bedded to lenticular mudstone with conspicuous laminated units. Porous, flat pebble conglomerate with rare shelter voids at very top. Irregular surface at 20.9 ft. Common moldic porosity (after mud clasts) in the flat pebble conglomerate.

Unit 5: 19.6-17.3 ft.
Olive gray silty, argillaceous dolostone. Primary depositional texture not apparent. Scattered intraclasts. Local deformation of beds. Sparse microstylolites. Sparse to common intercrystalline and vuggy porosity. Largest pore 5 millimeters, although pores 0.25 millimeters or smaller are more characteristic of the interval.

Unit 6: 17.3-13.3 ft.
Brownish gray and olive gray silty, slightly argillaceous dolostone. Primary depositional texture not apparent. Unit capped by microstylolites swarm. Top 0.4 ft. with abundant

intraclasts. Small void at 15.2 ft. filled with quartz silt and clay. Rare to sparse microstylolites. Rare to sparse pyrite. Excellent vuggy and intercrystalline porosity. Largest pore 0.5 millimeters.

Unit 7: 13.3-11.5 ft.
Brownish gray and olive gray silty argillaceous dolostone. Primary depositional texture not apparent. Largely (11.9-13.3 ft.) a brecciated unit with fault trace at the top. Pressure solution contacts between clasts. Apparently compressional deformation and oblique orientation of clasts at the base. No brecciation at the top, although beds undulate. No apparent porosity adjacent to fault. Rare vuggy porosity in brecciated portion. Largest pore 1 millimeter.

Unit 8: 11.5-3.4 ft.
Brownish gray and olive gray silty, argillaceous dolostone, rarely slightly calcitic. Although, deformation and diagenesis have obscured primary depositional fabric, it appears to be a "ribbon rock". Beds locally brecciated and often inclined. Beds often appear smeared or distorted by ductile deformation. Sparse pyrite. Common microstylolites. Rare calcite-filled fractures. Rare voids filled with saddle dolomite and calcite spar, are adjacent to the fault. Intercrystalline and vuggy porosity best developed proximal to fault trace.

Unit 9: 3.4-0.0 ft.
Olive gray, silty, argillaceous dolostone. Diagenesis have obscured primary depositional fabric. Minor deformation, but texture is, overall, homogenous. Rare clasts. No apparent porosity.

HOLE 6

Little Falls Formation

45.0-25.1 ft.

Little Falls-Tribes Hill Transitional Beds

25.1-24.3 ft.
Brownish gray, slightly argillaceous and slightly silty dolostone to dolomitic limestone at top. Thinly bedded mudstone. Some beds are lenticular, contorted and not continuous, probably reflecting early, soft sediment deformation. Rare burrows. Rare microstylolites. Rare pyrite.

Tribes Hill Formation

Unit 1: 24.3-23.7 ft.
Brownish gray, silty, argillaceous, slightly dolomitic limestone. Basal 0.2 ft. more clastic rich and dolomitic. Crinkly laminated mudstone, thinly bedded mudstone and rare packstone. Rare burrows. Numerous, thin silty, argillacous laminae. Rare lenticular lenses of gravel size intraclasts. Laminae fragmented *in situ* at base. Numerous, microstylolites which concentrate silt and clay. Rare pyrite.

Unit 2: 23.7-23.4 ft.
Olive gray, dolomitic limestone. Intraclast packstone to grainstone. Rounded very coarse sand and gravel sized well-rounded micritic intraclasts. Many intraclasts appear to have small post-depositional fractures. Intergranular (matrix) pores filled and replaced by dolomite and glauconite.

Unit 3: 23.4-21.9 ft.
Olive black silty, argillaceous, dolomitic limestone. I*n situ* breccia (pseudobreccia). Many laminated mudstone chips later tectonically fractured. Sparse cemented shelter voids associated with mudstone chips. Sparse compactional fracturing. Extensive bioturbation disrupts mudstone beds. Rare glauconite. Clay and silt generally as thin microstylolites. Rare pyrite.

Unit 4: 21.9-20.1 ft.
Olive black silty dolostone, with a sharp transition to an olive gray, silty dolomitic limestone (at 20.5 ft.). Bedded to lenticular bedded mudstone and, perhaps, fine peloidal grainstone at base. Sparse microstylolites. Fine cross-laminations near base. Sparse pyrite. Rare mudstone flat pebble conglomerate and cemented shelter voids at top. Rare pyrite.

Unit 5: 20.1-17.3 ft.
Olive black to olive gray silty, argillaceous, slightly dolomitic limestone. "Ribbon rock" and nodular fabric of interbedded limestone and silty, argillacous dolomitic

microstylolitic seams. Mudstone and rare packstone and grainstone. Capped by a planar surface (hardground?), on an intraclastic grainstone. Limestone generally less than 5 centimeters. Carbonate grains include peloids, intraclasts and echinoderms. Rare pyrite. Rare to sparse horizontal and vertical burrows, some geopetally filled with calcite spar. Rare echinoderm and trilobite fragments.

Unit 6: 16.5-17.3
Brownish gray and medium dark gray to olive gray, silty dolomitic limestone. Locally very silty and very dolomitic. Intraclastic-peloidal packstone and rare wackestone. Numerous hardgrounds. Rare stylolites and microstylolites. Rare to sparse pyrite. No visible porosity.

Unit 7: 17.3-12.9-ft.
Olive gray silty, argillaceous dolomitic limestone to calcitic dolostone. Perhaps a less distinct "ribbon rock" with fewer, conspicuous microstylolitic seams and thicker limestone interbeds. Locally nodular. Mudstone with rare, thin grainstone and packstone interbeds. Carbonate grains include peloids, gastropods, intraclasts, echinoderms, brachiopods and trilobites. Rare pyrite. Sparse, thin, discontinuous microstylolites except for abundance of microstylolites in mudstone near base and top of unit.

Unit 8: 12.9-0.0 ft.
Olive gray, silty, clayey slightly dolomitic limestone. "Ribbon rock" and nodular fabric of interbedded limestone and silty, clayey dolomitic microstylolitic seams. Limestone beds rarely greater than 10-15 millimeters. Limestone interbeds generally are wackestones and packstone. Many intraclasts are mudstone. Algal fragments (Ortonella?) are a conspicuous and common component. Trilobites, echinoderms, ostracods brachiopods, intraclasts, peloids are the most common carbonate grains. Some "intraclasts" may be the steinkerns of gastropods. Rare calcite-filled fractures.

Appendix 2. FIT's Fluid Inclusion Analyses

PB200: This sample consists of relatively coarse, possibly recrystallized matrix dolomite with very coarse saddle spar and late calcite spar. No visible liquid petroleum inclusions are identified. Possible non-fluorescent gas inclusions are observed in saddle spar, but these are small and difficult to image. These inclusions may have pyrobitumen coatings. None responded to micro-thermometric tests. Pyrobitumen may be present, and appears to post-date dolomite, but predate calcite.

Primary aqueous inclusions in early matrix dolomite have homogenization temperatures of 120-130°C and indeterminate salinities. Secondary or pseudo-secondary inclusions in early matrix calcite have homogenization temperatures of 80-95°C and salinities of 26-28 weight percent salt (estimated from the NaCl-$CaCl_2$-H_2O system). No aqueous inclusions could be found in late saddle dolomite, and possible gas inclusions did not respond to heat/cooling tests, as mentioned. Secondary or pseudo-secondary inclusions in late calcite cement have consistent homogenization temperatures of 65-75°C and salinities of 14.5-18.6 weight percent NaCl-equivalent.

PB201: This sample consists of relatively coarse zoned dolomite with minor, possibly partially dissolved, late calcspar. No visible liquid petroleum inclusions are identified. Abundant pyrobitumen is noted.

Primary aqueous inclusions in dolomite have homogenization temperatures of 105-132°C with a possible weak trend of higher temperature from core (105-120°C) to rim (120-132°C). Secondary or pseudo-secondary aqueous inclusions in dolomite have homogenization temperatures of 90-129°C. Salinities are uniformly very high at 26-30 weight percent salt (estimated from the NaCl-$CaCl_2$-H_2O system). No aqueous inclusions could be measured from late calcite.